



# **A surrogate model based on feature selection techniques and regression learners to improve soybean yield prediction in southern France**

David Camilo Corrales, Céline Schoving, Hélène Raynal, P Debaeke, Etienne-Pascal Journet, Julie Constantin

## **► To cite this version:**

David Camilo Corrales, Céline Schoving, Hélène Raynal, P Debaeke, Etienne-Pascal Journet, et al.. A surrogate model based on feature selection techniques and regression learners to improve soybean yield prediction in southern France. Computers and Electronics in Agriculture, 2022, 192, pp.106578. 10.1016/j.compag.2021.106578 . hal-03454504

**HAL Id: hal-03454504**

**<https://hal.science/hal-03454504>**

Submitted on 29 Nov 2021

**HAL** is a multi-disciplinary open access archive for the deposit and dissemination of scientific research documents, whether they are published or not. The documents may come from teaching and research institutions in France or abroad, or from public or private research centers.

L'archive ouverte pluridisciplinaire **HAL**, est destinée au dépôt et à la diffusion de documents scientifiques de niveau recherche, publiés ou non, émanant des établissements d'enseignement et de recherche français ou étrangers, des laboratoires publics ou privés.

# A surrogate model based on feature selection techniques and regression learners to improve soybean yield prediction in southern France

David Camilo Corrales <sup>a, b, \*</sup>, Céline Schoving <sup>c</sup>, Hélène Raynal <sup>a</sup>, Philippe Debaeke <sup>a</sup>, Etienne-Pascal Journet <sup>a, d</sup> and Julie Constantin <sup>a</sup>

<sup>a</sup> Université de Toulouse, INRAE, UMR AGIR, F-31326, Castanet-Tolosan, France

<sup>b</sup> Grupo de Ingeniería Telemática, Universidad del Cauca, Sector Tulcán, Popayán, Colombia

<sup>c</sup> Terres Inovia, Baziège, France

<sup>d</sup> Université de Toulouse, INRAE, CNRS, LIPME, F-31326, Castanet-Tolosan, France

\* Corresponding author. E-mail address: [davidcamilo.corralesmunoz@inrae.fr](mailto:davidcamilo.corralesmunoz@inrae.fr), [dcorrales@unicauca.edu.co](mailto:dcorrales@unicauca.edu.co)

## Abstract

Empirical and process-based models are currently used to predict crop yield at field and regional levels. A mechanistic model named STICS (Multidisciplinary Simulator for Standard Crops) has been used to simulate soybean grain yield in several environments, including southern France. STICS simulates at a daily step the effects of climate, soil and management practices on plant growth, development and production. In spite of good performances to predict total aboveground biomass, poor results were obtained for final grain yield. In order to improve yield prediction, a surrogate model was developed from STICS dynamic simulations, feature selection techniques and regression learners. STICS was used to simulate functional variables at given growth stages and over selected phenological phases. The most representative variables were selected through feature selection techniques (filter, wrapper and embedded), and a subset of variables were used to train the regression learners Linear regression (LR), Support vector regression (SVR), Back propagation neural network (BPNN), Random forest (RF), Least Absolute Shrinkage and Selection Operator (LASSO) and M5 decision tree. The subset of variables selected by wrapper method combined with regression models SVR ( $R^2 = 0.7102$ ; subset of variables = 6) and LR ( $R^2 = 0.6912$ ; subset of variables = 14) provided the best results. SVR and LR models improved significantly the soybean yield predictions in southern France in comparison to STICS simulations ( $R^2 = 0.040$ ).

**Keywords:** *STICS; regression learners; filter; wrapper; embedded*

## 1- Introduction

Soybean (*Glycine max* L.) is grown on 125 million ha worldwide, with a total average production of 340 million tons on the 2016-2020 period (Oil Word, 2020). On an absolute basis, soybean is the fourth most important grain crop after wheat, maize and rice. USA, Brazil, and Argentina are the three most producing countries, accounting collectively for 81 % of the global production (Grassini et al., 2021). EU-27 is a marginal producer (2.6 million tons, <0.8 % of world production), importing *ca.* 95 % of its soybean domestic needs as rich-protein GMO (Genetically Modified Organisms) and non-GMO meals for animal feed. In Europe, France is the second most important producer after Italy (186 500 ha in 2020), the two main producing

regions being South-West and Center-East parts with an increasing contribution of organically-grown production. One main objective in France is to achieve self-sufficiency at least in non-GMO soybean meals at 2025 horizon. Therefore, EU-27 members share a common objective: “*reducing markedly the dependency upon soybean imports by developing European production*”. Soybean crop requires few pesticides, no N-fertilizer and less irrigation than maize, results in low emissions of greenhouse gases, hence bringing environmental benefits. In addition, it could contribute as a summer crop to the diversification of winter cereal-based systems.

Grain yield in France slightly increased since the 80s (Terres Univia, 2021). In 2019, yields were 2.61 t.ha<sup>-1</sup> for France, 2.09 t.ha<sup>-1</sup> for all Europe, but 3.19, 3.18, and 3.33 t.ha<sup>-1</sup> for USA, Brazil and Argentina respectively (FAOSTAT, 2021). Climate change and its impacts on temperature, precipitation, and CO<sub>2</sub> concentration, but also on water resources available for irrigation, will certainly impact the future production (Porter et al., 2014; Guilpart et al., 2020; Kothari et al., 2020). In addition, expanding soybean growing areas northward and introducing new cropping systems (e.g. double cropping with cereals, rainfed or irrigated soybean, etc.) will change the potential and attainable grain yields.

Therefore predicting soybean yield in various environments and a range of cropping systems will be necessary to evaluate the ability of France and European countries to achieve their objectives in terms of protein self-sufficiency by growing more soybean in cropland. Modeling can be efficient in yield analysis and investigation of the limiting factors due to easy manufacturing, testing, applying, understanding and interpretation of results (Nehbandani et al., 2020).

Yield prediction models are based on historical or future climate data for evaluating production potentials; also, yield prediction models assimilate remote sensing information when applied to in-season prediction. Nowadays, both statistical and mechanistic approaches are used in agricultural modelling, especially for yield prediction. Statistical approaches search and explore the relations between data to explain the variables of interest whereas mechanistic models are based on the description of biophysical processes. Dynamic crop models simulate daily growth and development in relation with environmental resources and agricultural inputs; they allow the testing of functional hypotheses and the identification of potential constraints to crop growth and yield (Purcell & Roedel, 2019). However, mechanistic and statistical approaches can be combined in order to improve the crop modeling predictions (Casadebaig et al., 2011, 2020).

Statistical models from traditional Artificial Neural Networks (ANN) and Deep Learning (DL) have been used for soybean yield prediction. ANN models were proposed by (Kaul et al., 2005) in order to predict Maryland soybean yield at state, regional, and local levels. ANN were developed using historical yield data (1978–1998). Field-specific rainfall data and Soil Rating for Plant Growth (SRPG) values were used for each location. The work developed in (Maimaitijiang et al., 2020) estimated the soybean grain yield through multispectral images (information type: canopy spectral, structure, thermal and texture features) and DLN in Columbia, Missouri. A Convolutional Neural Network (CNN) for soybean yield prediction in 15 states of CONUS (United States) is proposed in (Sun et al., 2019). The model was trained by crop growth and environment variables, which include weather data, MODIS Land Surface Temperature data, and MODIS Surface Reflectance data. In Cachoeira do Sul, Brazil, a Multi-Layer Perceptron (MLP) was used to adjust a predictive model for estimating the yield of

soybean crop based on 9 vegetation indices (Eugenio et al., 2020). A soybean yield model was created by deep learning framework using CNN and recurrent neural networks (Khaki et al., 2020). Model was built based on environmental data and management practices from Corn Belt (including 13 states) in the United States. In southern Brazil different type of indices as Normalized Difference Vegetation Index (NVDI), Enhanced vegetation index (EVI), land surface temperature (LST) and precipitation were used to build a model using Long-Short Term Memory (LSTM), Neural Networks (Schwalbert et al., 2020). ANN was developed to evaluate the relative importance of predictor variables as vegetation indices (NDVI, red edge NDVI and simple ratio-SR) and elevation derived variables (slope, flow accumulation, aspect) for the prediction of soybean in Ontario, Canada (Kross et al., 2020).

Traditional regression models/analysis were used with the same purpose. Authors in (Stepanov et al., 2020) used backward stepwise in order to build a regression model in Khabarovsk, Russia. Several data sources were used as Moderate Resolution Imaging Spectroradiometer (MODIS), arable land mask and meteorological stations. The NDVI was used to improve soybean yield predictions using the flexible Fourier transform model in United States (Xu & Katchova, 2019). The objective was to explore the relationships between soybean yield and number of grains (NG) and thousand grains weight (TGW), generate equations to estimate yield in several countries in the years 2010 and 2019 (Wei & Molin, 2020). A regression analysis was developed by (Ma et al., 2001) in order to study the correlations between plant canopy reflectance and aboveground biomass for early prediction of soybean yield in Canada.

In addition, mechanistic models were calibrated in order to predict soybean yield. Authors in (Robertson & Carberry, 1998) used Agricultural Production Systems Simulator (APSIM) with aim to simulate the soybean yield. The model was tested on an independent set of experiments, from northern Australia, with factors such as cultivars, sowing date, irrigation, soil type, plant population density row spacing varying. The research proposed by (Jagtap & Jones, 2002) developed a procedure to simulate soybean yield and production by linking the CROPGRO-soybean model with a regional resolution (about a 50 km grid cell) database of weather, soils, management, and varieties in the state of Georgia over the 1974–1995 time period. The CROPGRO-Soybean model was calibrated to estimate potential yields and yield gaps of soybean for 21 locations regions in India (Bhatia et al., 2008). Authors in (Ovando et al., 2018) simulated soybean yield using a DSSAT model through weather data from Clouds and Earth's Radiant Energy System (CERES) and Tropic Rainfall Measurement Mission (TRMM) for 2006 – 2016 in Oliveros, Argentina. In (Battisti et al., 2017), the model for Nitrogen and Carbon in Agroecosystems (MONICA) was used to simulate soybean grain yield for 14 sites in Southern Brazil. The models CSM-CROPGRO-Soybean and STICS (Multidisciplinary Simulator for Standard Crops) were used to simulate soybean yield responses under near (2041–2070) and distant (2071–2100) future climate scenarios in eastern Canada (Jing et al., 2017).

The AgMip initiative started an inter-comparison of 10 soybean crop models at 5 locations in major global production areas with high quality observed data for calibration (Kothari et al., 2020). Among the tested models, STICS (Brisson et al., 2009), a widely used soil-plant crop model applied on a wide range of crops (305 papers in Web of Science), appeared as moderately performing with a prediction gap. Previous attempts to validate STICS on soybean concluded to good performance in aboveground biomass prediction but poor results on grain yield and protein concentration (Schoving, 2020). In eastern Canada, (Jégo et al., 2010) obtained scattered results for biomass, LAI and yield, with Root Mean Square Error (RMSE) from 23 to

38 %. Heretofore, this model has been used less in soybean crops, but encouraging results were recently obtained through proper calibration on pea and faba bean, two other grain legumes (Falconnier et al., 2019, 2020). In addition, STICS describes with a good accuracy the dynamics of water and nitrogen in soils and a module was introduced for considering explicitly  $N_2$ -fixation in legumes.

Improving the STICS prediction for soybean could imply a thorough calibration of the model and/or a deep re-examination of the underlying biophysical processes. The experimental data required for such an improvement could be insufficient. The data-driven modeling approach has emerged as an alternative to model the biophysical system purely from the data available. A data-driven model, also known as a meta-model or surrogate model, is a “model of the model” (Cui et al., 2016). A surrogate model is a statistical model trained from simulations/variables difficult to measure in field (e.g. leaf area index, aboveground crop biomass, N crop uptake, crop transpiration, etc.). The surrogate model can be deployed to replace or support the original biophysical simulation module to accurately approximate the simulation output. Figure 1 explains the interactions between surrogate and STICS model.

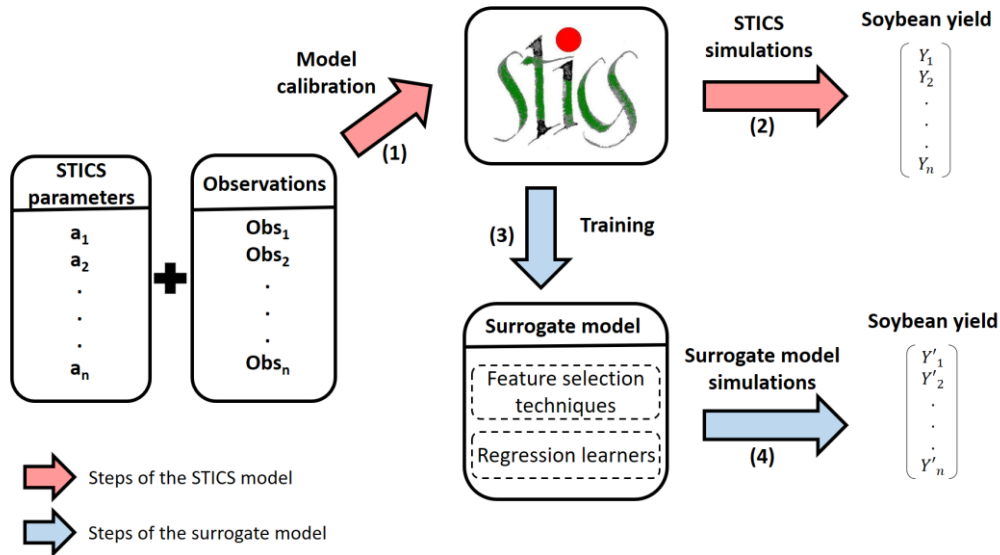


**Figure 1.** Steps of STICS and surrogate model to predict the soybean yield. The red arrows show the process of soybean yield simulations generated by STICS. (1) Parameters are calibrated and field observations are used to run STICS. (2) Soybean yield simulations  $Y_1, Y_2, \dots, Y_n$  generated by STICS. The blue arrows depict the steps to create the surrogate model. (3) The STICS simulations are used to select the relevant variables and train the surrogate model. (4) Soybean yield simulations  $Y'_1, Y'_2, \dots, Y'_n$  generated by the surrogate model.

In this sense, we proposed a surrogate model based on feature selection techniques and regression learners to predict soybean yield in southern France. The surrogate model is trained from the data produced by STICS simulations generated by (Schoving, 2020) (effects of climate, soil and management practices on dynamic variables of soybean crop functioning) to improve the prediction of final grain yield. This study progressed through three steps:

- Calculate crop variables at different phenological stages with STICS as evaluated by (Schoving, 2020) in southern France.
- Find the representative variables of soybean yield based on feature selection techniques.
- Build a regression model to predict soybean yield based on representative variables found by feature selection techniques.



## 2- Materials and methods

### Multidisciplinary Simulator for Standard Crops (STICS)

The STICS model simulates at a daily step the effects of climate, soil and management practices on plant growth, development and production (quantity and quality) and environmental impacts. The combination of these input variables is termed a USM (Unit of SiMulation). Each USM corresponds to one execution of the STICS model (Brisson et al., 1998). STICS can be tuned to a single crop, two intercropped or several successive crop cycles. STICS has been evaluated over a large data set for 15 different crops and different conditions of soil and climate in France (Coucheney et al., 2015).

In order to calibrate STICS, the crop files contain species parameters, ecophysiological options (e.g. effect of photoperiod and/or cold requirements on crop phenology, potential radiation use efficiency) and cultivar specific parameters (e.g. flowering precocity, maximum number of grains per m<sup>2</sup>). Crop temperature (calculated from weather variables) and photoperiod drive crop phenology. The model dynamically simulates (i) the development of the root system that takes up N and water according to root density over the whole soil profile and (ii) the establishment of the canopy that transpires water and intercepts light to produce the crop biomass (Brisson et al., 2009).

### Study area and datasets

The data used in this work were collected by (Schoving, 2020). Seventeen experimental sites were conducted during 2010-2018 from six regions in the south of France: Mauguio (2010), Béziers (2010 - 2012), Mondonville (2010 - 2014), Rivières (2010 - 2014), En Crambade (2013 - 2014) and Auzeville (2017 - 2018) as shown in Figure 2.



**Figure 2.** Locations in Southern France where experimental sites were conducted. Locations are depicted by red markers (Mauguio, Béziers, Mondonville, Rivières, En Crambade and Auzeville). This figure was created by Google Earth.

The eleven tested soybean varieties belonged to four maturity groups corresponding to different crop durations and potential yields: 000 (very early-maturing), 0, I and II (late-maturing). Three late-maturing varieties were tested in all experiments since 2010 (Ecudor, Santana, Isidor and Sarema). Detailed information on varieties and maturity groups are presented in Table A1 (Appendix A). Weather data were collected near to the experimental sites. Soil samples contain texture and physico-chemical analyzes. These data are essential to correctly initialize STICS with realistic values of soil moisture and mineral nitrogen (nitrate, ammonium). The water pressure of the soils was monitored in a micro-plot of Santana variety, at 30, 60 and 90 cm depth.

The dataset contains 227 simulation units (USM) created from combination of experimental sites, years and cropping practices (cultivar, water management and sowing date); We used the same training (105 USMs) and test (122 USMs) datasets as defined by (Schoving, 2020). The train-test split was defined based on the number of variables measured in field by experimental sites (variables such as phenology, biomass, leaf area index, grain yield and seed protein content). Most complete observations measured in field were selected to train the surrogate model while data with less observations were retained for the test set. We preprocessed 87 variables based on agronomist knowledge from a selection of 19 STICS state variables calculated daily by the model during its simulation (Table 1). The preprocessed variables concern either state variables at different crop phenology stages (Ilev: emergence, Idrp: grain filling onset, Iflo: flowering, Imat: physiological maturity), descriptive values (Cum: cumulative, Max: maximum, Avg: average) and thresholds set for variables as MinTemp (days MinTemp < 18°C), MaxTemp (days MaxTemp > 28°C), Swfac (days Swfac < 0.6) and Inn (days Inn < 0.6). The soybean grain yield is represented by variable Mafruit (Table 1; dependent variable).

STICS variables	Units	Description
Nbgrmax	m <sup>-2</sup>	Maximal grain number
Stlevdrp	°C.days	Heat sum from emergence to grain filling onset
Stflodrp	°C.days	Heat sum from flowering to grain filling onset
Stdrrpmat	°C.days	Heat sum from grain filling onset to physiological maturity
Masec(n)	t.ha <sup>-1</sup>	Aboveground crop biomass
Lai(n)	m <sup>2</sup> .m <sup>-2</sup>	Leaf area index
Qnplante	kg.ha <sup>-1</sup>	Cumulative amount of N taken up by the crop
Qfix	kg.ha <sup>-1</sup>	Cumulative amount of N fixed by the crop
Zrac	m	Water excess stress index on roots
Jul	Julian day	Julian day
Raint	MJ.m <sup>-2</sup>	Photosynthetic active radiation intercepted by the canopy
Etp(n)	mm.d <sup>-1</sup>	Daily potential evapotranspiration
Precip	mm.d <sup>-1</sup>	Precipitation
Ep	mm.d <sup>-1</sup>	Daily actual transpiration
AvgTemp	°C	Average air temperature
MinTemp	°C	Minimum air temperature
MaxTemp	°C	Maximum air temperature
Swfac	0-1	Stomatal water stress index
Inn	0-2	Nitrogen nutrition index
Mafruit	t.ha <sup>-1</sup>	Biomass of harvested organs (grain yield)

**Table 1.** Variables used from Multidisciplinary Simulator for Standard Crops (STICS).

For instance, preprocessed variables computed by phenology stages as *Lai(n)\_Iflo* variable indicates the leaf area index *Lai(n)* at flowering (*Iflo*). Other variables are expressed over phenophases, for example *Precip\_cum\_Iflo-Imat* represents the cumulative precipitation (*Precip*) between two phenological stages: flowering (*Iflo*) and physiological maturity (*Imat*). In addition, we define variables by phenophases and thresholds as *Days\_MinTemp\_18\_Ilev-Imat* variable which indicates the number of days when minimum temperature was less than 18°C between emergence and physiological maturity stages. Table 2 presents a summary of preprocessed variables from STICS by stages or phases, descriptive values and thresholds. Table A2 (Appendix A) lists all of the preprocessed variables.

STICS variables	Stages or phases	Descriptive value	Threshold	Number of variables
Nbgrmax	-	-	-	1
Stlevdrp	-	-	-	1
Stflodrp	-	-	-	1
Stdrpmat	-	-	-	1
Masec(n)	Iflo, Idrp, Imat	-	-	3
Lai(n)	Iflo, Idrp, Imat	-	-	3
Qnplante	Iflo, Idrp, Imat	-	-	3
Qfix	Iflo, Idrp, Imat	-	-	3
Zrac	Iflo, Idrp, Imat	-	-	3
Jul	Ilev-Imat, Iflo-Imat, Idrp-Imat, Iflo-Idrp	Cum	-	4
Raint	Ilev-Imat, Iflo-Imat, Idrp-Imat, Iflo-Idrp	Cum	-	4
Etp(n)	Ilev-Imat, Iflo-Imat, Idrp-Imat, Iflo-Idrp	Cum	-	4
Precip	Ilev-Imat, Iflo-Imat, Idrp-Imat, Iflo-Idrp	Cum	-	4
Ep	Ilev-Imat, Iflo-Imat, Idrp-Imat, Iflo-Idrp	Cum	-	4
AvgTemp	Ilev-Imat, Iflo-Imat, Idrp-Imat, Iflo-Idrp	Avg	-	4
MinTemp	Ilev-Imat, Iflo-Imat, Idrp-Imat, Iflo-Idrp	Avg	# days MinTemp < 18	8
MaxTemp	Ilev-Imat, Iflo-Imat, Idrp-Imat, Iflo-Idrp	Avg, Max	# days MaxTemp > 28	12
Swfac	Ilev-Imat, Iflo-Imat, Idrp-Imat, Iflo-Idrp	Avg, Min	# days Swfac < 0.6	12
Inn	Ilev-Imat, Iflo-Imat, Idrp-Imat, Iflo-Idrp	Avg, Min	# days Inn < 0.6	12

**Table 2.** Preprocessed variables from Multidisciplinary Simulator for Standard Crops (STICS). STICS variables were preprocessed by crop phenology stages (Ilev: emergence, Idrp: grain filling onset, Iflo: flowering, Imat: physiological maturity), descriptive values (Cum: cumulative, Max: maximum, Avg: average) and thresholds (MinTemp, MaxTemp, Swfac and Inn). Last column (Var) corresponds to number of variables processed from a STICS, phenology stages, descriptive values and thresholds. Table A2 (Appendix A) lists all of the preprocessed variables.

In order to create an interpretable soybean yield model with a minimum number of variables, we applied feature selection techniques to previous dataset based on three approaches: filter, embedded and wrapper.

## Feature selection techniques

Feature selection is the process (automatic or manual) of selecting a subset of relevant variables which contribute most to learner (Corrales et al., 2018). Feature selection techniques can be grouped in three categories:

- **Filter methods** are based only on the intrinsic properties of the data (Solorio-Fernández et al., 2020). Filter method computes an importance value between one independent variable and the dependent variable. Variables with highest importance values are selected based on user criteria. Filter methods are usually computationally less expensive than embedded and wrapper methods. We used classical feature selection



methods based on Pearson (Pearson, 1920) and Spearman (Spearman, 1961) coefficients and Information Gain (Shannon, 1948). In order to explain the statistical coefficients, independent variable is named  $X$  and dependent variable  $Y$ .

- **Pearson coefficient** measures the linear correlation between two variables. If both variables are linearly dependent, then their correlation coefficient is close to  $\pm 1$ . If the variables are uncorrelated, the correlation coefficient is 0 (Pearson, 1920). When Pearson coefficient is used as filter method only positive values are considered following the equation (1):

$$r = \left| \frac{\sum_{i=1}^n cov(x_i, y_i)}{\sum_{i=1}^n \sigma x_i \sigma y_i} \right| \quad (1)$$

Where  $x_i$  and  $y_i$  are the  $i^{th}$  observations of independent and dependent variable respectively;  $cov$  corresponds to covariance and  $\sigma$  indicates the standard deviation of  $x$  and  $y$ .

- **Spearman coefficient** through a monotonic function measures the correlation between two variables (Spearman, 1961). A monotonic function is defined as function which is either entirely increasing or decreasing. It is similar to Pearson coefficient except that it operates on the ranks of the data rather than the raw data (Gauthier, 2001). The Spearman correlation rank is defined by equation (2):

$$\rho = 1 - \frac{6 \sum_{i=1}^n d_i^2}{n(n^2 - 1)} \quad (2)$$

Where  $d_i$  is the difference between ranks for each  $x_i, y_i$  data pair and  $n$  is the number of data pairs.

- **Entropy-based information gain** discretizes the independent variable and subsequently the entropy is computed between  $x$  and continuous  $y$  variable (Yang et al., 2010) by equation (3):

$$InfoGain = H(y) + H(x) - H(y, x) \quad (3)$$

Where  $H(x)$  and  $H(y)$  correspond to Shannon's Entropy for  $x$  and  $y$  variables.  $H(y, x)$  is a joint Shannon's Entropy for a variable  $y$  with a condition to  $x$ . Detailed explanation of Shannon's Entropy is explained in (Shannon, 1948).

- **Embedded methods** integrate the variables selection as part of training process into learner (Guyon & Elisseeff, 2003). We used as embedded methods the learners Random Forest (Breiman, 2001), M5 decision tree (Quinlan, 1992) and Least Absolute Shrinkage and Selection Operator (Tibshirani, 1996).
- **Wrapper methods** selects a subset of variables according to performance criteria (regression tasks, measure of errors as mean absolute error, mean square error, root square mean error; classification tasks measures as accuracy, precision, overall, recall,

etc.) of a learner (Guyon & Elisseeff, 2003). In this paper, we use the method Recursive Feature Elimination (Guyon et al., 2002).

## Regression learners

In order to predict soybean yield in southern France crops, we used regression learners from different families of algorithms. They are explained briefly below.

- **Linear regression (LR)** explains the relationship between dependent variable and one or more independent variables by fitting a linear equation to observed data (Prion & Haerling, 2020). Coefficients multiply the values of dependent values; the coefficient signs represent the direction of the relationship between a dependent variable and the independent variable.
- **Support vector regression (SVR)** is based on same principles as Support Vector Machine (Vapnik, 1995). SVR determines a regression function in the feature space considering only data points within the decision boundary lines called support vectors. In nonlinear data, a kernel function is used in order to transform the feature space into a linear hyperplane (Brereton & Lloyd, 2010).
- **Back propagation neural network (BPNN)** calculates the gradient of the error function with respect to the weights of the neural network (Rumelhart et al., 1986). The computed error is propagated in a backward manner from one layer to the other until the minimum Mean Squared Error (MSE) is attained and weights can be modified accordingly (Deshwal et al., 2020).

In addition, we used each of Random forest, Least Absolute Shrinkage and Selection Operator and M5 decision tree as both an embedded method and a wrapper.

- **Random forest (RF)** builds several decision trees using a different bootstrap sample of data training set (Breiman, 2001). The decision trees are built using CART learner (Breiman et al., 1984). In regression tasks, RF final prediction is obtained by averaging the results of all the CART trees.
- **Least Absolute Shrinkage and Selection Operator (LASSO)** is a linear regression method which imposes a bound on the  $L_1$ -norm of the regression coefficients, resulting in coefficient shrinkage (Tibshirani, 1996). LASSO adds a  $L_1$  penalty equal to the absolute value of the magnitude of coefficients (Equation 1). Variables are discarded when the coefficients take values equal to zero. Larger penalties are expressed by coefficient values closer to zero. The objective function for finding the minimum is shown by Equation (4):

$$\text{minimize } \beta_0, \beta \left( \frac{1}{2N} \sum_{i=1}^N (y_i - \beta_0 - x_i^T \beta)^2 + \lambda \sum_{j=1}^p |\beta_j| \right) \quad (4)$$

Where  $N$  is the total number of observations,  $\lambda$  is a nonnegative regularization parameter corresponding to one value of Lambda,  $y_i$  is the dependent variable,  $p$  is the

number of independent variables  $x_i = (x_{i1}, \dots, x_{ip})^T$ ,  $\beta_0$  is the intercept, and  $\beta_j$  are the coefficients (Shi et al., 2020).

- **M5** is a conventional decision tree composed by different nodes such as root, intermediates and leaves (Quinlan, 1992). Root and intermediate nodes are chosen over the dependent variable that maximizes the expected error reduction as a function of the standard deviation of output parameter (Wang & Witten, 1996). Leaves nodes predict the dependent variable through linear regression functions; they are fitted from data that follows one branch between root and leaf node.

### 3- Results

This section reports the subset of variables selected by feature selection methods and the evaluation of soybean yield models built from selected variables.

#### 3.1 Feature selection

##### 3.1.1 Filter methods

Filter methods were computed through R 'mlr' package (Bischl et al., 2016). With aim to create simple models with great explanatory predictive power with a minimum number of features, we defined two criteria to select the variables: (i) top-15 of variables with highest importance values for each filter method; (ii) variables selection by threshold based on importance values of top-15. Regarding to Pearson and Spearman coefficients, we selected the features with importance value greater than or equal to 0.6. Concerning to entropy-based information gain, we selected the features with importance value greater than or equal to 0.4. We defined these thresholds following the “conventional interpretation of the correlation coefficients” proposed in (Schober et al., 2018). Values between 0.60 - 0.79 are defined as “moderately correlated” and coefficient values between 0.70 – 0.89 are interpreted as “strongly correlated”. Table 3 shows Top-15 of soybean variables selected by filter methods (Appendix B contains the entire ranking).

Pos	Pearson coefficient		Spearman coefficient		Entropy-based information gain	
	Variable	Importance	Variable	Importance	Variable	Importance
1	Masec(n)_Imat	0.7923	Lai(n)_Imat	0.7699	Lai(n)_Imat	0.5929
2	Lai(n)_Imat	0.7726	Masec(n)_Imat	0.7311	Masec(n)_Imat	0.5875
3	Qnplante_Idrp	0.7710	Qnplante_Idrp	0.7137	Qnplante_Imat	0.5515
4	Qnplante_Imat	0.7523	Masec(n)_Idrp	0.7003	Ep_cum_Idrp-Imat	0.4223
5	Masec(n)_Idrp	0.7334	Ep_cum_Iflo-Imat	0.6886	Qfix_Imat	0.4072
6	Ep_cum_Idrp-Imat	0.6819	Ep_cum_Idrp-Imat	0.6734	Inn_min_Iflo-Idrp	0.3799
7	Qfix_Imat	0.6805	Qnplante_Imat	0.6714	Inn_avg_Iflo-Idrp	0.3652
8	Ep_cum_Iflo-Imat	0.6650	Ep_cum_Ilev-Imat	0.6456	Ep_cum_Iflo-Imat	0.3486
9	Raint_cum_Idrp-Imat	0.6326	Lai(n)_Idrp	0.6439	Days_Swfac_0.6_Iflo-Imat	0.3443
10	Lai(n)_Idrp	0.6292	Raint_cum_Idrp-Imat	0.6288	Inn_avg_Ilev-Imat	0.3400
11	AvgTemp_avg_Idrp-Imat	0.6157	Swfac_min_Idrp-Imat	0.6160	Inn_avg_Iflo-Imat	0.3380
12	Swfac_avg_Iflo-Imat	0.6088	Swfac_min_Iflo-Imat	0.6136	Masec(n)_Idrp	0.3300
13	MinTemp_avg_Idrp-Imat	0.5937	AvgTemp_avg_Idrp-Imat	0.6081	Qnplante_Idrp	0.3285
14	Ep_cum_Ilev-Imat	0.5842	Swfac_min_Ilev-Imat	0.6009	Raint_cum_Idrp-Imat	0.3080
15	Days_Swfac_0.6_Iflo-Imat	0.5811	MinTemp_avg_Idrp-Imat	0.5977	Days_Swfac_0.6_Iflo-Idrp	0.3025

Table 3. Top-15 of variables selected by filter methods: Pearson, Spearman and entropy-based information gain.

In this sense, 12 and 14 variables were selected by Pearson and Spearman respectively. The variables *Lai(n)\_Imat*, *Masec(n)\_Imat*, *Qnplante\_Imat*, *Ep\_cum\_Idrp-Imat* and *Qfix\_Imat* were selected by entropy-based information gain. The subdatasets with the selected variables by filter methods were used to train the regression learners presented in Section 2. Besides, RF, LASSO and M5 decision tree act as regression learners and feature selection techniques due these learners are considered embedded methods. In other words, RF, LASSO and M5 are trained with subset of variables selected by filter methods and subsequently the embedded methods/learners select a new subset of variables in the training process into learner. The results are presented in Table 5.

### 3.1.2 Embedded methods

We used as embedded methods the learners: Random forest, Least Absolute Shrinkage and Selection Operator and M5 decision tree. The variable selection process for each one is explained below.

#### Random Forest

Random Forest (RF) gathers a set of CART trees in order to obtain the soybean yield prediction by averaging the results of all of trees. We used R packages 'randomForest' to create RF model and 'randomForestExplainer' (Liaw & Wiener, 2002) to design multi-way plot shown in Figure 3. Five hundred CART trees were built (ntree parameter) as result, 42 variables were sampled as candidates at each split. The multi-way plot focuses on three importance measures that derive from the structure of trees in the forest: (i) the mean\_min\_depth variable refers to the depth of first split on the variable to the top of the tree; (ii) the times\_a\_root variable measures the number of times a variable is set as top of a decision tree. Figure 3 presents multi-way plot for first 15 relevant variables.

*Lai(n)\_Imat* was the most used variable as top split criterion (148 times) followed by *Masec(n)\_Imat* (67 times) and *Ep\_cum\_Iflo-Imat* (58 times). Variables as *Qfix\_Iflo* and *Precip\_cum\_Idrp-Imat* were never used as top of decision trees and they have the longest distance (mean minimum depth of 6.728 and 6.398 respectively) to the top of decision trees considered less associated with the dependent variable *Mafruit*. Other variables as *Qfix\_Idrp*, *Lai(n)\_Iflo* and *Precip\_cum\_Iflo-Idrp* can be considered as intermediate nodes of the trees (times\_a\_root = 0) with mean minimum depth less than *Precip\_cum\_Idrp-Imat* and *Qfix\_Iflo* (mean\_min\_depth = 4.856, 5.045 and 5.297 respectively).

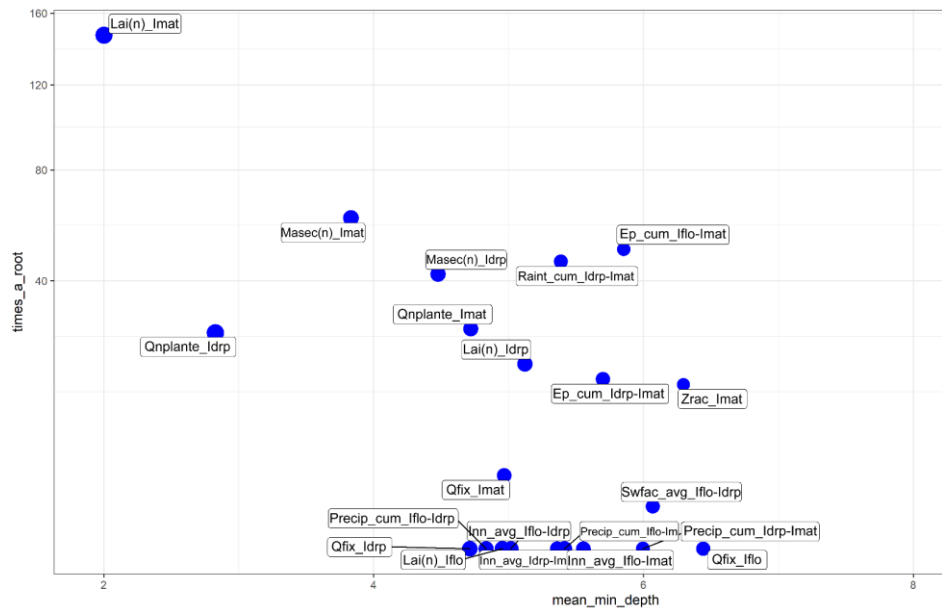


**Figure 3.** Multi-way plot between two measures of importance: mean\_min\_depth (x-axis) and times\_a\_root (y-axis). First 15 relevant variables are depicted. X-axis correspond to mean depth of first split on the variable, y-axis the number of trees in which the root is split on the variable.

## Least Absolute Shrinkage and Selection Operator

We used the R package 'caret' to build LASSO model (Kuhn, 2008). Root Mean Square Error (RMSE) was used to select the optimal model using the smallest value. LASSO model was run with parameters fraction = 0.1 and lambda = 0.01 (Equation 1). The LASSO model set the regression coefficients of 21 variables to zero by imposing the L1 penalty. Table C1 (Appendix C) contains the regression coefficients of 66 variables calculated by LASSO.

## M5 decision tree

M5 was built by R package 'RWeka' (Hornik et al., 2009). The construction of M5 tree is based on recursive splitting of the standard deviation of *Mafruit* (dependent variable) that reach a node as a measure of the error at the node. The variable that maximizes the expected error reduction is selected for splitting at the node. The expected reduction of the error is obtained as a result of testing each variable at that node. To remove the problem of over fitting, M5 uses a method to prune back the over grown tree. Figure 4 shows the structure of the pruned M5 tree to predict the soybean yield (*Mafruit*) regarding the thirteen selected variables (Table 4). Left branches show conditions below the node threshold, for example, if the top node  $Lai(n)_{Imat} \leq 1.103$  and if  $Inn\_avg\_Iflo\_Idrp \leq 0.769$ , the linear model LM 1 must be selected. Thirty-seven nodes were created including nineteen linear models as decision rules. We defined 3 observations as minimum number at the leaf node. Appendix C contains the linear models generated by M5.

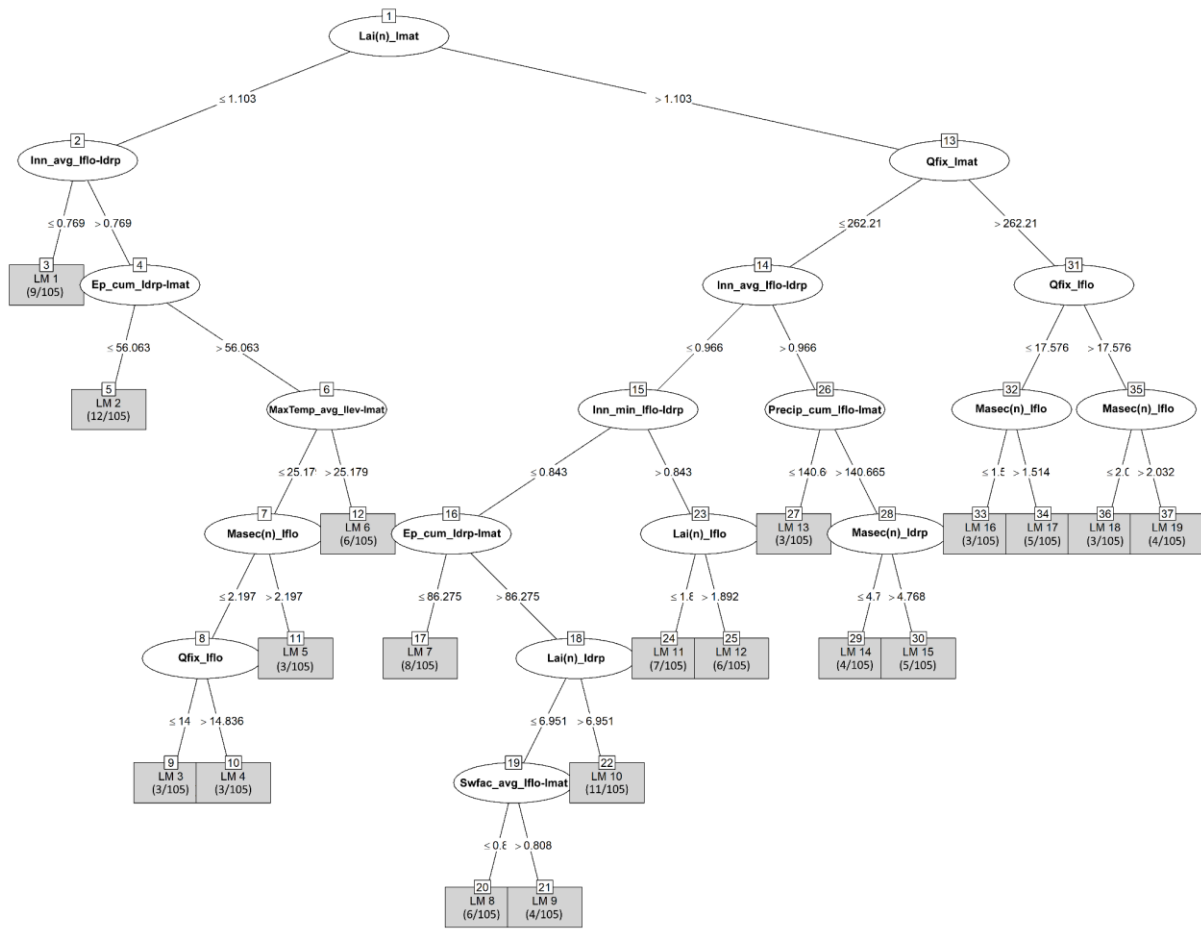


**Figure 4.** M5 pruned decision tree. Thirteen variables were selected and 19 decision rules (linear regressions) were created. At the leaf node, the number in parenthesis corresponds to observations for each linear regression.

### 3.1.3 Wrapper methods

A greedy algorithm named Recursive Feature Elimination (RFE) was used as wrapper method (Kohavi & John, 1997; Guyon et al., 2002). RFE selects a subset of variables to improve a learner performance by removing the least important features. This process is repeated recursively (based on backward elimination) until the optimal number of features is obtained. The recursive step plays a key role due the relative importance of each variable can change substantially over a different subset of variables during the backward elimination process (particularly for highly correlated variables) (Granitto et al., 2006). We used the RFE version coded in R package 'caret' (Kuhn, 2008). Six learners were selected (explained in section 2) to determine the performance of subsets of variables selected by RFE shown in Table 4. The variables subset selection were conducted through lowest Mean Absolute Error obtained by learners. Recursive Feature Elimination selected all of the variables for RF model. The variables subset for remaining models are less than 17.

Learner	Variables	Selected variables	RMSE
LR	<i>MaxTemp_avg_Idrp-Imat, Qnplante_Idrp, Masec(n)_Imat, Ep_cum_Idrp-Imat, Lai(n)_Imat, Raint_cum_Idrp-Imat</i>	6	0.5865
SVR	<i>Lai(n)_Imat, Masec(n)_Imat, Qnplante_Idrp, Qnplante_Imat, Masec(n)_Idrp, Ep_cum_Iflo-Imat, Ep_cum_Idrp-Imat,</i>	14	0.6750



	<i>Ep_cum_Ilev-Imat, Qfix_Imat, Zrac_Imat, Zrac_Idrp, Lai(n)_Idrp, Raint_cum_Idrp-Imat, MaxTemp_avg_Idrp-Imat</i>		
BPNN	<i>Lai(n)_Imat, Masec(n)_Imat, Qnplante_Idrp, Qnplante_Imat, Masec(n)_Idrp, Ep_cum&gt;Iflo-Imat, Ep_cum_Idrp-Imat, Qfix_Imat, Zrac_Imat, Zrac_Idrp, Ep_cum_Ilev-Imat, Lai(n)_Idrp, Raint_cum_Idrp-Imat, MaxTemp_avg_Idrp-Imat, Swfac_min_Ilev-Imat, Swfac_min&gt;Iflo-Imat</i>	16	1.294
RF	All variables were selected	87	0.4639
LASSO	<i>Lai(n)_Imat, Masec(n)_Imat, Qnplante_Idrp, Qnplante_Imat, Masec(n)_Idrp, Ep_cum&gt;Iflo-Imat, Ep_cum_Idrp-Imat, Qfix_Imat, Ep_cum_Ilev-Imat, Zrac_Idrp, Zrac_Imat, Raint_cum_Idrp-Imat, Lai(n)_Idrp, MinTemp_avg_Idrp-Imat, MaxTemp_avg_Idrp-Imat, Swfac_min&gt;Iflo-Imat</i>	16	6.141e-01
M5	<i>Lai(n)_Imat, Inn_avg_Idrp&gt;Iflo, Ep_cum_Idrp-Imat, MaxTemp_avg_Ilev-Imat, Masec(n)_Iflo, Qfix&gt;Iflo, Qfix_Imat, Inn_min&gt;Iflo-Idrp, Lai(n)_Idrp, Swfac_avg&gt;Iflo-Imat, Lai(n)_Iflo, Precip_cum&gt;Iflo-Imat, Masec(n)_Idrp</i>	13	0.5465

**Table 4.** Subset of variables selected by Recursive Feature Elimination (RFE) and base learners: Linear Regression (LR), Support Vector Regression (SVR), M5 decision tree, Random Forest (RF) and Backpropagation Neural Network (BPNN). Learner performance is based on Root Mean Square Error (RMSE).

Concerning time complexity, RFE is slower than filter and embedded methods, since RFE needs to evaluate performance criteria for each iteration besides the computational cost of the model training. In this sense, learners based on linear models as LR and LASSO obtained much less computational cost (59.42 and 137.53 seconds) than BPNN, RF and M5 (1421.25, 1268.27 and 1033.52 seconds). In contrast to Support Vector Regression which imposed considerable computational cost (5271.56 seconds) due to margin maximization to find the support vectors and nonlinear transformations of the feature space (Yu et al., 2003). Figure 5 presents the time complexity of the variables subset selection by Recursive Feature Elimination and base learners. Wrapper methods were run on Windows 10 comprised of Intel Core i5-774HQ CPU 2.80GHz – 16GB RAM based on sequential computing.

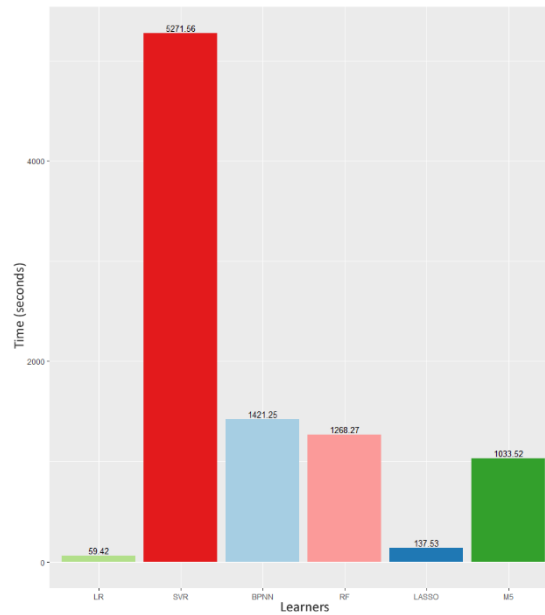


**Figure 5.** Time complexity to select subset of variables by Recursive Feature Elimination (RFE) and base learners: Linear Regression (LR), Support Vector Regression (SVR), M5 decision tree, Random Forest (RF) and Backpropagation Neural Network (BPNN).

### 3.2 Regression models

In order to examine the performance of subset of variables selected by feature selection methods, we used traditional statistical criteria to estimate the prediction accuracy of regression learners as Coefficient of determination ( $R^2$ ), Mean Square Error (MSE), Root Mean Square Error (RMSE) and Mean Absolute Error (MAE). The metric  $R^2$  was adopted to measure the correlation of the observed and predicted values.

Regression learners were trained with 105 observations and evaluated with 122 examples (explained in section 2). Table 5 presents the results of regression learners trained with subset of variables selected by feature selection methods. The underlined values correspond to statistical criteria obtained by best two learners and feature selection method.

Feature selection approach	Feature selection method	SC	Learners					
			LR	SVR	BPNN	RF	LASSO	M5
Filter	Pearson correlation	$R^2$	0.6185	0.6389	0.1837	0.3487	0.6274	0.6193
		MSE	0.9085	0.6539	2.1301	1.0325	0.7250	0.9211
		RMSE	0.9531	0.8086	1.4595	1.0161	0.8514	0.9597
		MAE	0.7227	0.6267	1.2375	0.8422	0.6552	0.7258
		No. Selected Variables	12	12	12	12	12	12
	Spearman correlation	$R^2$	0.5890	0.6394	0.1841	0.3463	0.6101	0.6276
		MSE	1.0418	0.6948	1.4388	1.0818	0.8167	0.6776
		RMSE	1.0207	0.8335	1.1995	1.0401	0.9037	0.8231
		MAE	0.7889	0.6551	1.0158	0.8505	0.6862	0.6397
		No. Selected Variables	14	14	14	14	14	14
	Entropy-based information gain	$R^2$	0.3974	0.3916	0.2701	0.2622	0.3961	0.2502
		MSE	0.9479	1.0085	4.0698	1.1859	0.9554	1.2713
		RMSE	0.9736	1.0042	2.0173	1.0890	0.9774	1.1275
		MAE	0.7951	0.8215	1.7373	0.8815	0.7975	0.9212
		No. Selected Variables	5	5	5	5	5	5
Embedded	Learners: RF, LASSO and M5	$R^2$	-	-	-	0.5020	0.1249	0.4010
		MSE	-	-	-	0.8300	6.1841	0.9466
		RMSE	-	-	-	0.9110	2.4867	0.9729
		MAE	-	-	-	0.7258	1.9206	0.7802
		No. Selected Variables	-	-	-	42	66	87
Wrapper	Recursive Feature Elimination (RFE)	$R^2$	<u>0.6912</u>	<u>0.7102</u>	0.1829	0.5020	0.6718	0.4010
		MSE	<u>0.4807</u>	<u>0.4170</u>	1.4916	0.8300	0.4760	0.9466
		RMSE	<u>0.6933</u>	<u>0.6458</u>	1.2213	0.9110	0.6899	0.9729
		MAE	<u>0.5469</u>	<u>0.5230</u>	0.9746	0.7258	0.5747	0.7802
		No. Selected Variables	6	14	16	87	16	13

**Table 5.** Results of regression learners trained with subset of variables selected by feature selection methods. Validation dataset (Section 2) was used to evaluate the regression learners. Statistical criteria (SC) used to estimate the performance of regression learners: Coefficient of determination ( $R^2$ ), Mean Square Error (MSE), Root Mean Square Error (RMSE) and Mean Absolute Error (MAE). The underlined values correspond to statistical criteria obtained by best two learners and feature selection method.

According to filter methods, Pearson, Spearman and Entropy coefficients selected 12, 14 and 5 variables respectively (Section 3). The regression learners LR, SVR and BPNN were trained with subset of variables selected by filter methods; SVR obtained the best results with subset of feature selected by Pearson coefficient ( $R^2 = 0.6389$ , MSE = 0.6539, RMSE = 0.8086 and MAE = 0.6267). Regression learners RF, LASSO and M5 decision tree act as ensemble

approaches for feature selection due these learners are considered embedded methods as well. In other words, embedded methods were trained with subset of variables selected by filter methods. Subsequently, embedded methods select a new subset of variables in the training process into learner. However, the ensemble of filter and embedded methods do not improve the performance obtained by SVR trained with subset of variables chosen by Pearson coefficient.

The number of variables selected by two embedded methods were higher respecting to others feature selection approaches. Random Forest and LASSO selected 87 and 66 variables respectively, whereas M5 decision Tree 13 variables (Section 3). Random Forest reached the best performance in the ensemble methods ( $R^2 = 0.5020$ ,  $MSE = 0.8300$ ,  $RMSE = 0.9110$  and  $MAE = 0.7258$ ), however RF does not overcome the performance obtained by SVR and Pearson coefficient in the filter methods.

Concerning to wrapper method, Recursive Feature Elimination selected 6, 14 and 16 variables for LR, SVR and BPNN. SVR achieved the best results compared to all of combination of feature selection approaches and learners ( $R^2 = 0.7102$ ,  $MSE = 0.4170$ ,  $RMSE = 0.6458$  and  $MAE = 0.5230$ ). Remain of learners that work as ensemble feature selection among wrapper and embedded methods (RF, LASSO and M5 decision tree), RFE proposes different subset of variables created in the backward elimination process. The embedded methods are tested with subset of variables proposed by wrapper method and they select a new subset of variables in the training process into learner. The best subset of variables are selected regarding to performance criteria of the embedded method. LASSO trained with 16 variables selected by RFE (Table 4) reached the best results ( $R^2 = 0.6718$ ,  $MSE = 0.4760$ ,  $RMSE = 0.6899$  and  $MAE = 0.5747$ ) compared to RF and M5 of the wrapper method. Besides, RFE improve the performance of LASSO compared to LASSO's version of filter and embedded.

In summary, the wrapper methods RFE-SVR ( $R^2 = 0.7102$ ,  $MSE = 0.4170$ ,  $RMSE = 0.6458$  and  $MAE = 0.5230$ ) and RFE-LR ( $R^2 = 0.6912$ ,  $MSE = 0.4807$ ,  $RMSE = 0.6933$  and  $MAE = 0.5469$ ) achieved the best results from validation dataset. Figure 6 depicts the scatter plots of observed vs simulated soybean yield values by RFE-SVR and RFE-LR.

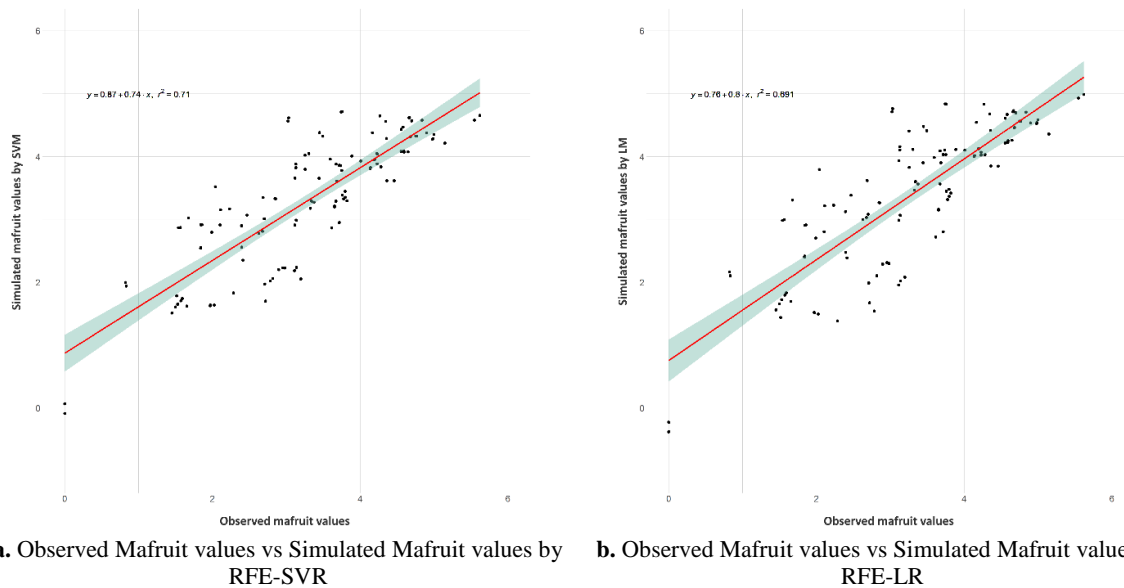


**Figure 6.** Scatter plot of observed (x-axis) vs simulated (y-axis) Mafruit values by RFE-SVR (14 variables) and RFE-LR (6 variables)

For real values of soybean yield equal to zero, RFE-SVR and RFE-LR predict negative soybean values or close to zero. RFE-SVR simulates Mafruit values equal to 0.066, -0.086 and -0.085 for 3 observations where Mafruit = 0 of the validation dataset (Béziers in 2011 with maturity group I in varieties Isidor, Santana and maturity group II in Ecudor variety). Similarly, LR-RFE predicts -0.227, -0.379 and -0.378 for same observations of validation dataset.

### 3.3 Comparative study

In order to demonstrate the performance of RFE-SVR and RFE-LR, we compared both regression models against STICS simulations developed in (Schoving, 2020). The soybean yield model proposed by Schoving was calibrated with the same training set as presented in section 2. Table 6 shows the results of RFE-SVR, RFE-LR and STICS models evaluated from validation dataset (Section 2).

Models	Statistical criteria	
	R <sup>2</sup>	RMSE
RFE-SVR	0.710	0.645
RFE-LR	0.691	0.693
(Schoving, 2020)	0.040	1.320

**Table 6.** Comparison of Support Vector Regression and Linear Regression (LR) trained with subset of variables selected by Recursive Feature Selection (RFS) vs soybean yield model proposed by (Schoving, 2020). Validation dataset (Section 2) was used to evaluate the models. Statistical criteria used to estimate the performance of models: Coefficient of determination (R<sup>2</sup>) and Root Mean Square Error (RMSE).

The two regression models explained around 70 % of the grain yield variation and they achieved half of RMSE values obtained for STICS simulations developed in (Schoving, 2020). Although total aboveground biomass was correctly simulated by (Schoving, 2020) ( $r^2 = 0.64$ ), final grain yield of semi-indeterminate and indeterminate soybean cultivars was poorly represented (Table 6;  $r^2 = 0.04$ ). This is probably because STICS uses the standard formalism of wheat and maize crops to simulate the final grain yield in soybean.

## 4- Discussion

Feature selection methods are relevant in order to reduce the computational complexity and improve the model generalization ability (Maldonado & Weber, 2009). High dimensional variables impose a high computational cost and a high cost of data acquisition. On the other hand, a low-dimensional representation reduces the risk of overfitting (Famili et al., 1997; Liu & Zheng, 2006). The value added by applying feature selection techniques is to determinate a subset of available variables to build a good model, which is a combinatorial problem in the number of original variables (Wolsey & Nemhauser, 1999; Guyon & Elisseeff, 2003).

With this rationale, we used popular filter, embedded and wrapper methods in order to select the relevant variables to predict soybean yield.

Filter methods are independent of any learners and they are based on performance evaluation metrics calculated directly from the data. We used two correlation-based filters (Pearson and Spearman) followed by a measure based on information theory (Information Gain). Figure 7 presents Venus diagram of top-15 variables selected by filter methods. Correlation-based filters selected twelve same variables. The correlations found by Pearson and Spearman are equivalent to rank the common twelve variables; whereas Pearson inspects straight connections, Spearman evaluates monotonic connections (regardless of whether direct or not) (Thirumalai et al., 2017). However, of the three filter methods share less features in common (eight variables) due to

entropy-based information is designed to observe the amount of information gained between two discrete variables, and dataset used contains only numeric variables.

The principle of embedded methods (feature selection as part of the training process) is to reduce the computation time taken up for testing several subsets of variables which is done in wrapper methods (Chandrashekar & Sahin, 2014). In this work, the number of variables selected by RF and LASSO were higher. LASSO selected 66 variables and Random Forest all of the initial variable set. Although M5 decision Tree selected less variables (13), the results were worse than RF ( $R^2 = 0.4010$ ,  $MSE = 0.9466$ ,  $RMSE = 0.9729$  and  $MAE = 0.7802$ ). Embedded methods showed an improvement when they were used as ensemble approaches of filter and wrapper techniques.

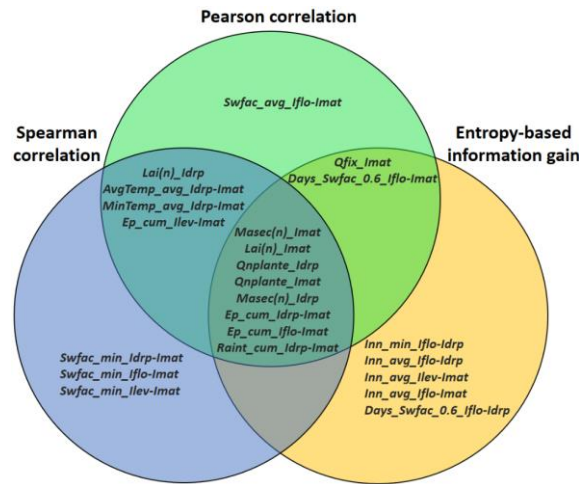


**Figure 7.** Venus diagram of top-15 variables selected by filter methods: Pearson, Spearman and Entropy-based information

Wrapper methods are widely recognized and considered a superior alternative for two reasons: (i) they evaluate variables iteratively with respect to performance learner. Therefore, variables selected by wrapper approach are more likely to suit the learner (Kohavi & John, 1997); (ii) wrapper approaches evaluate variables jointly and are effective in capturing intrinsic relationships such as interactions among multiple variables (Freitas, 2001). However computational cost is high, even for learners that exhibit a moderate complexity, the number of iterations required by the search of subset variables is high, especially as more complex search strategies are used (Talavera, 2005). In this paper, we used a dataset with few observations (105 instances) but it contains a large number of features (87 variables). Recursive Feature Elimination through SVR and LR learners reached the best performance. RFE-SVR and RFE-LR are recommended to be used as surrogate models to predict soybean yield in southern France. Concerning to time complexity, the lowest time was obtained by RFE-LR (59.42 seconds) against RFE-SVR (5271.56 seconds).

On the other hand, Support Vector Regression and Linear Regression belong different type of learners. SVR is considered a black-box model whereas LR an interpretable model (Loyola-González, 2019). SVR builds a hyperplane or set of hyperplanes in a high-dimensional space, which are very hard to explain and to be understood by experts in practical applications (Rudin, 2019). LR generates a linear equation to explain the correlation among variables in a language close to a human expert.

In this sense, RFE-LR is represented by the following linear equation:

$$Mafruit = -0.3095*MaxTemp\_avg\_Idrp\_Imat + 0.0148*Qnplante\_Idrp + 0.0057*Masec(n)\_Imat + 0.0066*Ep\_cum\_Idrp\_Imat + 0.0458 *Lai(n)\_Imat + 0.0008*Raint\_cum\_Idrp\_Imat + 8.5049 \quad (9)$$

RFE-LR model explains biologically the higher leaf area duration during grain filling through the increase of grain yield (*Mafruit*) with aboveground biomass at maturity (*Masec(n)\_Imat*), precipitation amount (*Raint\_cum\_Idrp-Imat*), cumulative crop transpiration during grain filling (*Ep\_cum\_Idrp-Imat*), the mineral nitrogen accumulated by the plants at the onset of grain filling (*Qnplante\_Idrp*) and residual leaf area index at maturity (*Lai(n)\_Imat*). All these variables demonstrate that radiation, water and nitrogen resources are highly representative variables of soybean grain yield. Further, the high temperatures may affect crop photosynthesis and grain filling (*MaxTemp\_avg\_Idrp-Imat*) which is in accordance with our knowledge of soybean physiology (Grassini et al., 2021).

## Acknowledgments

This research was supported by Horizon 2020 SusCrop-ERA-NET Cofound on Sustainable Crop Production: LegumeGap project (2019-2021) “Increasing productivity and sustainability of European plant protein production by closing the grain legume yield gap”: <https://www.suscrop.eu/projects-first-call/legumegap>

## REFERENCES

- Battisti, R., Parker, P. S., Sentelhas, P. C., & Nendel, C. (2017). Gauging the sources of uncertainty in soybean yield simulations using the MONICA model. *Agricultural Systems*, 155, 9–18.  
<https://doi.org/10.1016/j.agsy.2017.04.004>
- Bhatia, V. S., Singh, P., Wani, S. P., Chauhan, G. S., Rao, A. V. R. K., Mishra, A. K., & Srinivas, K. (2008). Analysis of potential yields and yield gaps of rainfed soybean in India using CROPGRO-Soybean model. *Agricultural and Forest Meteorology*, 148(8), 1252–1265.  
<https://doi.org/10.1016/j.agrformet.2008.03.004>
- Bischl, B., Lang, M., Kotthoff, L., Schiffner, J., Richter, J., Studerus, E., Casalicchio, G., & Jones, Z. M. (2016). mlr: Machine Learning in R. *The Journal of Machine Learning Research*, 17(1), 5938–5942.
- Breiman, L. (2001). Random forests. *Machine Learning*, 45(1), 5–32.
- Breiman, L., Friedman, J. H., Olshen, R. A., & Stone, C. J. (1984). *Classification and regression trees*. CERN Document Server; Wadsworth & Brooks/Cole Advanced Books & Software.  
<https://cds.cern.ch/record/2253780>



583 Brereton, R. G., & Lloyd, G. R. (2010). Support Vector Machines for classification and regression.  
584 *Analyst*, 135(2), 230–267. <https://doi.org/10.1039/B918972F>

585 Brisson, N., Launay, M., Mary, B., & Beaudoin, N. (2009). *Conceptual basis, formalisations and*  
586 *parameterization of the STICS crop model*. Editions Quae.

587 Brisson, N., Mary, B., Ripoche, D., Jeuffroy, M. H., Ruget, F., Nicoullaud, B., Gate, P., Devienne-Barret,  
588 F., Antonioletti, R., & Durr, C. (1998). *STICS: a generic model for the simulation of crops and*  
589 *their water and nitrogen balances. I. Theory and parameterization applied to wheat and corn*.

590 Casadebaig, P., Debaeke, P., & Wallach, D. (2020). A new approach to crop model calibration:  
591 Phenotyping plus post-processing. *Crop Science*, 60(2), 709–720.  
592 <https://doi.org/10.1002/csc2.20016>

593 Casadebaig, P., Guilioni, L., Lecoeur, J., Christophe, A., Champolivier, L., & Debaeke, P. (2011).  
594 SUNFLO, a model to simulate genotype-specific performance of the sunflower crop in  
595 contrasting environments. *Agricultural and Forest Meteorology*, 151(2), 163–178.  
596 <https://doi.org/10.1016/j.agrformet.2010.09.012>

597 Chandrashekar, G., & Sahin, F. (2014). A survey on feature selection methods. *Computers & Electrical*  
598 *Engineering*, 40(1), 16–28. <https://doi.org/10.1016/j.compeleceng.2013.11.024>

599 Corrales, D. C., Lasso, E., Ledezma, A., & Corrales, J. C. (2018). Feature selection for classification  
600 tasks: Expert knowledge or traditional methods? *Journal of Intelligent & Fuzzy Systems*, 34(5),  
601 2825–2835.

602 Coucheney, E., Buis, S., Launay, M., Constantin, J., Mary, B., de Cortázar-Atauri, I. G., Ripoche, D.,  
603 Beaudoin, N., Ruget, F., & Andrianarisoa, K. S. (2015). Accuracy, robustness and behavior of  
604 the STICS soil–crop model for plant, water and nitrogen outputs: Evaluation over a wide  
605 range of agro-environmental conditions in France. *Environmental Modelling & Software*, 64,  
606 177–190.

607 Cui, C., Hu, M., Weir, J. D., & Wu, T. (2016). A recommendation system for meta-modeling: A meta-  
608 learning based approach. *Expert Systems with Applications*, 46, 33–44.  
609 <https://doi.org/10.1016/j.eswa.2015.10.021>

610 Deshwal, D., Sangwan, P., & Kumar, D. (2020). A Language Identification System using Hybrid  
611 Features and Back-Propagation Neural Network. *Applied Acoustics*, 164, 107289.  
612 <https://doi.org/10.1016/j.apacoust.2020.107289>

613 Eugenio, F. C., Grohs, M., Venancio, L. P., Schuh, M., Bottega, E. L., Ruoso, R., Schons, C., Mallmann,  
614 C. L., Badin, T. L., & Fernandes, P. (2020). Estimation of soybean yield from machine learning  
615 techniques and multispectral RPAS imagery. *Remote Sensing Applications: Society and*  
616 *Environment*, 20, 100397. <https://doi.org/10.1016/j.rsase.2020.100397>

617 Falconnier, G. N., Journet, E.-P., Bedoussac, L., Vermue, A., Chlébowski, F., Beaudoin, N., & Justes, E.  
618 (2019). Calibration and evaluation of the STICS soil-crop model for faba bean to explain  
619 variability in yield and N<sub>2</sub> fixation. *European Journal of Agronomy*, 104, 63–77.  
620 <https://doi.org/10.1016/j.eja.2019.01.001>

621 Falconnier, G. N., Vermue, A., Journet, E.-P., Christina, M., Bedoussac, L., & Justes, E. (2020).  
622 Contrasted response to climate change of winter and spring grain legumes in southwestern  
623 France. *Field Crops Research*, 259, 107967. <https://doi.org/10.1016/j.fcr.2020.107967>

624 Famili, A., Shen, W.-M., Weber, R., & Simoudis, E. (1997). Data preprocessing and intelligent data  
625 analysis. *Intelligent Data Analysis*, 1(1), 3–23.

626 FAOSTAT. (2021). *Food and agriculture organization of the united nations—Crops*.  
627 <http://www.fao.org/faostat/en/#data/QC>

628 Freitas, A. A. (2001). Understanding the crucial role of attribute interaction in data mining. *Artificial*  
629 *Intelligence Review*, 16(3), 177–199.

630 Gauthier, T. D. (2001). Detecting trends using Spearman’s rank correlation coefficient. *Environmental*  
631 *Forensics*, 2(4), 359–362.

632 Granitto, P. M., Furlanello, C., Biasioli, F., & Gasperi, F. (2006). Recursive feature elimination with  
633 random forest for PTR-MS analysis of agroindustrial products. *Chemometrics and Intelligent*  
634 *Laboratory Systems*, 83(2), 83–90.

635 Grassini, P., Cafaro La Menza, N., Rattalino Edreira, J. I., Monzón, J. P., Tenorio, F. A., & Specht, J. E.  
636 (2021). Chapter 8—Soybean. In V. O. Sadras & D. F. Calderini (Eds.), *Crop Physiology Case*  
637 *Histories for Major Crops* (pp. 282–319). Academic Press. [https://doi.org/10.1016/B978-0-12-](https://doi.org/10.1016/B978-0-12-819194-1.00008-6)  
638 [819194-1.00008-6](https://doi.org/10.1016/B978-0-12-819194-1.00008-6)

639 Guilpart, N., Iizumi, T., & Makowski, D. (2020). Data-driven yield projections suggest large  
640 opportunities to improve Europe’s soybean self-sufficiency under climate change. *BioRxiv*,  
641 2020.10.08.331496. <https://doi.org/10.1101/2020.10.08.331496>

642 Guyon, I., & Elisseeff, A. (2003). An introduction to variable and feature selection. *Journal of Machine*  
643 *Learning Research*, 3(Mar), 1157–1182.

644 Guyon, I., Weston, J., Barnhill, S., & Vapnik, V. (2002). Gene Selection for Cancer Classification using  
645 Support Vector Machines. *Machine Learning*, 46(1), 389–422.  
646 <https://doi.org/10.1023/A:1012487302797>

647 Hornik, K., Buchta, C., & Zeileis, A. (2009). Open-source machine learning: R meets Weka.  
648 *Computational Statistics*, 24(2), 225–232. <https://doi.org/10.1007/s00180-008-0119-7>

649 Jagtap, S. S., & Jones, J. W. (2002). Adaptation and evaluation of the CROPGRO-soybean model to  
650 predict regional yield and production. *Agriculture, Ecosystems & Environment*, 93(1), 73–85.  
651 [https://doi.org/10.1016/S0167-8809\(01\)00358-9](https://doi.org/10.1016/S0167-8809(01)00358-9)

652 Jégo, G., Pattey, E., Bourgeois, G., Morrison, M. J., Drury, C. F., Tremblay, N., & Tremblay, G. (2010).  
653 Calibration and performance evaluation of soybean and spring wheat cultivars using the  
654 STICS crop model in Eastern Canada. *Field Crops Research*, 117(2), 183–196.  
655 <https://doi.org/10.1016/j.fcr.2010.03.008>

656 Jing, Q., Huffman, T., Shang, J., Liu, J., Pattey, E., Morrison, M., Jégo, G., & Qian, B. (2017). Modelling  
657 soybean yield responses to seeding date under projected climate change scenarios. *Canadian*  
658 *Journal of Plant Science*. <https://doi.org/10.1139/cjps-2017-0065>

659 Kaul, M., Hill, R. L., & Walthall, C. (2005). Artificial neural networks for corn and soybean yield  
660 prediction. *Agricultural Systems*, 85(1), 1–18. <https://doi.org/10.1016/j.agsy.2004.07.009>

661 Khaki, S., Wang, L., & Archontoulis, S. V. (2020). A CNN-RNN Framework for Crop Yield Prediction.  
662 *Frontiers in Plant Science*, 10. <https://doi.org/10.3389/fpls.2019.01750>

663 Kohavi, R., & John, G. H. (1997). Wrappers for feature subset selection. *Artificial Intelligence*, 97(1),  
664 273–324. [https://doi.org/10.1016/S0004-3702\(97\)00043-X](https://doi.org/10.1016/S0004-3702(97)00043-X)

665 Kothari, K., Salmeron, M., Battisti, R., Boote, K., Archontoulis, S., Confalone, A., Constantin, J., Cuadra  
666 Sanatiago, V., Debaeke, P., Faye, B., Grant, B., Hoogen-Boom, G., Jing, Q., Michael Van Der  
667 10, L., Macena, F., Marin, F., Nehbandani, A., Nendel, C., Larry, P., ... Viera Nilson, A. (2020,  
668 February). First Soybean Multi-model Sensitivity Analysis to CO<sub>2</sub>, Temperature, Water, and  
669 Nitrogen. *ICROP2020: Second International Crop Modelling Symposium*, Montpellier.  
670 <https://hal.inria.fr/hal-02950318>

671 Kross, A., Znoj, E., Callegari, D., Kaur, G., Sunohara, M., Lapen, D. R., & McNairn, H. (2020). Using  
672 Artificial Neural Networks and Remotely Sensed Data to Evaluate the Relative Importance of  
673 Variables for Prediction of Within-Field Corn and Soybean Yields. *Remote Sensing*, 12(14),  
674 2230. <https://doi.org/10.3390/rs12142230>

675 Kuhn, M. (2008). Building predictive models in R using the caret package. *Journal of Statistical*  
676 *Software*, 28(5), 1–26.

677 Liaw, A., & Wiener, M. (2002). Classification and regression by randomForest. *R News*, 2(3), 18–22.

678 Liu, Y., & Zheng, Y. F. (2006). FS\_SFS: A novel feature selection method for support vector machines.  
679 *Pattern Recognition*, 39(7), 1333–1345.

680 Loyola-González, O. (2019). Black-Box vs. White-Box: Understanding Their Advantages and  
681 Weaknesses From a Practical Point of View. *IEEE Access*, 7, 154096–154113.  
682 <https://doi.org/10.1109/ACCESS.2019.2949286>

683 Ma, B. L., Dwyer, L. M., Costa, C., Cober, E. R., & Morrison, M. J. (2001). Early Prediction of Soybean  
684 Yield from Canopy Reflectance Measurements. *Agronomy Journal*, 93(6), 1227–1234.  
685 <https://doi.org/10.2134/agronj2001.1227>

686 Maimaitijiang, M., Sagan, V., Sidike, P., Hartling, S., Esposito, F., & Fritschi, F. B. (2020). Soybean yield  
687 prediction from UAV using multimodal data fusion and deep learning. *Remote Sensing of*  
688 *Environment*, 237, 111599. <https://doi.org/10.1016/j.rse.2019.111599>

689 Maldonado, S., & Weber, R. (2009). A wrapper method for feature selection using Support Vector  
690 Machines. *Information Sciences*, 179(13), 2208–2217.  
691 <https://doi.org/10.1016/j.ins.2009.02.014>

692 Nehbandani, A., Soltani, A., Nourbakhsh, F., & Dadrasi, A. (2020). Estimating crop model parameters  
693 for simulating soybean production in Iran conditions. *OCL*, 27, 58.  
694 <https://doi.org/10.1051/ocl/2020057>

695 Oil Word. (2020). *The OIL WORLD ANNUAL encyclopedia*.  
696 <https://www.oilworld.biz/t/publications/annual>

697 Ovando, G., Sayago, S., & Bocco, M. (2018). Evaluating accuracy of DSSAT model for soybean yield  
698 estimation using satellite weather data. *ISPRS Journal of Photogrammetry and Remote*  
699 *Sensing*, 138, 208–217. <https://doi.org/10.1016/j.isprsjprs.2018.02.015>

700 Pearson, K. (1920). Notes on the History of Correlation. *Biometrika*, 13(1), 25–45.  
701 <https://doi.org/10.2307/2331722>

702 Porter, J. R., Xie, L., Challinor, A. J., Cochrane, K., Howden, S. M., Iqbal, M. M., Lobell, D. B., &  
703 Travasso, M. I. (2014). *Food security and food production systems*.

704 Prion, S. K., & Haerling, K. A. (2020). Making Sense of Methods and Measurements: Simple Linear  
705 Regression. *Clinical Simulation in Nursing*, 48, 94–95.  
706 <https://doi.org/10.1016/j.ecns.2020.07.004>

707 Purcell, L. C., & Roekel, R. J. V. (2019). Simulating Soybean Yield Potential under Optimum  
708 Management. *Agrosystems, Geosciences & Environment*, 2(1), 190029.  
709 <https://doi.org/10.2134/age2019.04.0029>

710 Quinlan, J. R. (1992). Learning with continuous classes. *5th Australian Joint Conference on Artificial*  
711 *Intelligence*, 92, 343–348.

712 Robertson, M. J., & Carberry, P. S. (1998). Simulating growth and development of soybean in APSIM.  
713 *Proceedings, 10th Australian Soybean Conference*, 130–136.  
714 [https://publications.csiro.au/rpr/pub?list=BRO&pid=procite:e5446cf7-51a2-4606-a660-](https://publications.csiro.au/rpr/pub?list=BRO&pid=procite:e5446cf7-51a2-4606-a660-28dadebf68d)  
715 [28dadebf68d](https://publications.csiro.au/rpr/pub?list=BRO&pid=procite:e5446cf7-51a2-4606-a660-28dadebf68d)

716 Rudin, C. (2019). Stop explaining black box machine learning models for high stakes decisions and use  
717 interpretable models instead. *Nature Machine Intelligence*, 1(5), 206–215.  
718 <https://doi.org/10.1038/s42256-019-0048-x>

719 Rumelhart, D. E., Hinton, G. E., & Williams, R. J. (1986). Learning representations by back-propagating  
720 errors. *Nature*, 323(6088), 533–536.

721 Schober, P., Boer, C., & Schwarte, L. A. (2018). Correlation Coefficients: Appropriate Use and  
722 Interpretation. *Anesthesia and Analgesia*, 126(5), 1763–1768.  
723 <https://doi.org/10.1213/ANE.0000000000002864>

724 Schoving, C. (2020). *Analyse écophysiologique et modélisation dynamique des interactions génotype x*  
725 *environnement x conduite de culture chez le soja* [PhD Thesis, Université fédérale Toulouse  
726 Midi-Pyrénées]. <http://www.theses.fr/s164533>

727 Schwalbert, R. A., Amado, T., Corassa, G., Pott, L. P., Prasad, P. V. V., & Ciampitti, I. A. (2020).  
728 Satellite-based soybean yield forecast: Integrating machine learning and weather data for



729 improving crop yield prediction in southern Brazil. *Agricultural and Forest Meteorology*, 284,  
730 107886. <https://doi.org/10.1016/j.agrformet.2019.107886>

731 Shannon, C. E. (1948). A mathematical theory of communication. *The Bell System Technical Journal*,  
732 27(3), 379–423.

733 Shi, X., Wang, K., Cheong, T. S., & Zhang, H. (2020). Prioritizing driving factors of household carbon  
734 emissions: An application of the LASSO model with survey data. *Energy Economics*, 92,  
735 104942. <https://doi.org/10.1016/j.eneco.2020.104942>

736 Solorio-Fernández, S., Martínez-Trinidad, J. Fco., & Carrasco-Ochoa, J. A. (2020). A Supervised Filter  
737 Feature Selection method for mixed data based on Spectral Feature Selection and  
738 Information-theory redundancy analysis. *Pattern Recognition Letters*, 138, 321–328.  
739 <https://doi.org/10.1016/j.patrec.2020.07.039>

740 Spearman, C. (1961). *The Proof and Measurement of Association Between Two Things* (p. 58).  
741 Appleton-Century-Crofts. <https://doi.org/10.1037/11491-005>

742 Stepanov, A., Dubrovin, K., Sorokin, A., & Aseeva, T. (2020). Predicting Soybean Yield at the Regional  
743 Scale Using Remote Sensing and Climatic Data. *Remote Sensing*, 12(12), 1936.  
744 <https://doi.org/10.3390/rs12121936>

745 Sun, J., Di, L., Sun, Z., Shen, Y., & Lai, Z. (2019). County-Level Soybean Yield Prediction Using Deep  
746 CNN-LSTM Model. *Sensors*, 19(20), 4363. <https://doi.org/10.3390/s19204363>

747 Talavera, L. (2005). An evaluation of filter and wrapper methods for feature selection in categorical  
748 clustering. *International Symposium on Intelligent Data Analysis*, 440–451.

749 Terres Univia. (2021). *Plantes riches en protéines* (Chiffres Clés 2020, p. 24). Chiffres Clés 2020.  
750 <http://www.terresunivia.fr/documentation-presse/chiffres-cles/chiffres-cles>

751 Thirumalai, C., Chandhini, S. A., & Vaishnavi, M. (2017). Analysing the concrete compressive strength  
752 using Pearson and Spearman. *2017 International Conference of Electronics, Communication  
753 and Aerospace Technology (ICECA)*, 2, 215–218.

754 Tibshirani, R. (1996). Regression shrinkage and selection via the lasso. *Journal of the Royal Statistical*  
755 *Society: Series B (Methodological)*, 58(1), 267–288.

756 Vapnik, V. (1995). *The nature of statistical learning theory*. Springer science & business media.

757 Wang, Y., & Witten, I. H. (1996). *Induction of model trees for predicting continuous classes*.

758 Wei, M. C. F., & Molin, J. P. (2020). Soybean Yield Estimation and Its Components: A Linear  
759 Regression Approach. *Agriculture*, 10(8), 348.

760 Wolsey, L. A., & Nemhauser, G. L. (1999). *Integer and combinatorial optimization* (Vol. 55). John  
761 Wiley & Sons.

762 Xu, C., & Katchova, A. L. (2019). Predicting Soybean Yield with NDVI Using a Flexible Fourier  
763 Transform Model. *Journal of Agricultural and Applied Economics*, 51(3), 402–416.  
764 <https://doi.org/10.1017/aae.2019.5>

765 Yang, P., Zhou, B. B., Zhang, Z., & Zomaya, A. Y. (2010). A multi-filter enhanced genetic ensemble  
766 system for gene selection and sample classification of microarray data. *BMC Bioinformatics*,  
767 11(1), S5. <https://doi.org/10.1186/1471-2105-11-S1-S5>

768 Yu, H., Yang, J., & Han, J. (2003). Classifying large data sets using SVMs with hierarchical clusters.  
769 *Proceedings of the Ninth ACM SIGKDD International Conference on Knowledge Discovery and*  
770 *Data Mining*, 306–315.

771

## APPENDIX A

Experimental site	Year	Maturity group	Variety	Planting date	Water management	Soil	Observed variables
Auzeville	2017	000, I, II	Blancas, Ecudor, Santana, Isidor, Sultana, RGT, Shouna	80, 130	IRR, DRY	Clay, Loam	LAI, BNF, AGPN, AGB, GY, GNC, Oil
	2018	000, I, II	Blancas, Ecudor, Santana, Isidor, ES, Pallador, Sultana, RGT, Shouna	114, 155	IRR, DRY	Silty, Clay, Loam	BNF, AGPN, AGB, GY, GNC, Oil, roots depth
Béziers	2010	I, II	Isidor, Sumatra, Ecudor, Fukui, S109554	55, 76, 112	IRR	Loam	GY
	2011	0, I, II	Sarema, Isidor, Ecudor	67, 96, 132	IRR	Loam	GY
	2012	0, I, II	Sarema, Isidor, Ecudor	76, 103, 131	IRR	Silt, Loam	GY, GNC
En Crambade	2013	I, II	Isidor, Santana, Ecudor	74, 115	IRR, DRY	Clay	LAI, BNF, AGPN, AGB, GY, GNC, Oil
	2014	I, II	Isidor, Santana, Ecudor	73, 120	IRR, DRY	Clay	LAI, BNF, AGPN, AGB, GY, GNC, Oil
Mauguio	2010	I, II	Isidor, Sumatra, Ecudor, Fukui, S109554	74, 98, 145	IRR	Clay, Loam	GY
Mondonville	2010	I, II	Isidor, Sumatra, Ecudor, Fukui, S109554	61, 92, 138	IRR	Silt, Loam	GY
	2011	0, I, II	Sarema, Isidor, Ecudor	80, 102, 124	IRR	Silt, Loam	GY
	2012	I, II	Isidor, Ecudor	76, 97, 124	IRR	Silt, Loam	GY, GNC
	2013	I, II	Isidor, Santana, Ecudor	81, 147	IRR, DRY	Silt, Loam	LAI, BNF, AGPN, AGB, GY, GNC, Oil
	2014	I, II	Isidor, Santana, Ecudor	126	IRR, DRY	Silt, Loam	LAI, BNF, AGPN, AGB, GY, GNC, Oil
Rivières	2010	I, II	Isidor, Sumatra, Ecudor, Fukui, S109554	62, 99	IRR	Clay, Loam	GY
	2011	0, I, II	Sarema, Isidor, Ecudor	70, 102, 131	IRR	Clay, Loam	GY
	2012	I, II	Isidor, Ecudor	76, 108, 138	IRR	Clay, Loam	GY, GNC
	2013	I, II	Isidor, Santana, Ecudor	81, 126	IRR, DRY	Clay, Loam	LAI, BNF, AGPN, AGB, GY, GNC, Oil
	2014	I, II	Isidor, Santana, Ecudor	77, 126	IRR, DRY	Clay, Loam	LAI, BNF, AGPN, AGB, GY, GNC, Oil

**Table A1.** Dataset description of seventeen experimental sites during 2010-2018 from six regions in the south of France. The dataset contains 227 simulation units (USM) created from combination of experimental sites, years and cropping practices (cultivar, water management and sowing date). LAI: Leaf area index (m<sup>2</sup>.m<sup>-2</sup>), BNF: fixed nitrogen (kg.ha<sup>-1</sup>), AGPN: Total nitrogen (kg.ha<sup>-1</sup>), AGB: Biomass of aerial parts (t.ha<sup>-1</sup>), GY: Grain yield (t.ha<sup>-1</sup>), GNC: Nitrogen concentration in the grains (%), Oil: percentage of oil (%), roots depth: rooting depth (cm). Source: (Schoving, 2020) .

Table A2 lists all of the preprocessed variables from STICS basic variables, crop phenology stages, descriptive values and thresholds.

#	Variable	#	Variable	#	Variable
1	Nbgmax	30	Etp(n)_cum_Idrp-Imat	59	MaxTemp_max>Iflo-Idrp
2	Stlevdrp	31	Etp(n)_cum>Iflo-Idrp	60	Days_MaxTemp_28_Ilev-Imat
3	Stflodrp	32	Precip_cum_Ilev-Imat	61	Days_MaxTemp_28>Iflo-Imat
4	Stdrpmat	33	Precip_cum>Iflo-Imat	62	Days_MaxTemp_28_Idrp-Imat
5	Masec(n)_Iflo	34	Precip_cum_Idrp-Imat	63	Days_MaxTemp_28>Iflo-Idrp
6	Masec(n)_Idrp	35	Precip_cum>Iflo-Idrp	64	Swfac_avg_Ilev-Imat
7	Masec(n)_Imat	36	Ep_cum_Ilev-Imat	65	Swfac_avg>Iflo-Imat
8	Lai(n)_Iflo	37	Ep_cum>Iflo-Imat	66	Swfac_avg_Idrp-Imat
9	Lai(n)_Idrp	38	Ep_cum_Idrp-Imat	67	Swfac_avg>Iflo-Idrp
10	Lai(n)_Imat	39	Ep_cum>Iflo-Idrp	68	Swfac_min_Ilev-Imat
11	Qnplante>Iflo	40	AvgTemp_avg_Ilev-Imat	69	Swfac_min>Iflo-Imat
12	Qnplante_Idrp	41	AvgTemp_avg>Iflo-Imat	70	Swfac_min_Idrp-Imat
13	Qnplante_Imat	42	AvgTemp_avg_Idrp-Imat	71	Swfac_min>Iflo-Idrp
14	Qfix>Iflo	43	AvgTemp_avg>Iflo-Idrp	72	Days_Swfac_0.6_Ilev-Imat
15	Qfix_Idrp	44	MinTemp_avg_Ilev-Imat	73	Days_Swfac_0.6>Iflo-Imat
16	Qfix_Imat	45	MinTemp_avg>Iflo-Imat	74	Days_Swfac_0.6_Idrp-Imat
17	Zrac>Iflo	46	MinTemp_avg_Idrp-Imat	75	Days_Swfac_0.6>Iflo-Idrp
18	Zrac_Idrp	47	MinTemp_avg>Iflo-Idrp	76	Inn_avg_Ilev-Imat
19	Zrac_Imat	48	Days_MinTemp_18_Ilev-Imat	77	Inn_avg>Iflo-Imat
20	Jul_cum_Ilev-Imat	49	Days_MinTemp_18>Iflo-Imat	78	Inn_avg_Idrp-Imat
21	Jul_cum>Iflo-Imat	50	Days_MinTemp_18_Idrp-Imat	79	Inn_avg>Iflo-Idrp
22	Jul_cum_Idrp-Imat	51	Days_MinTemp_18>Iflo-Idrp	80	Inn_min_Ilev-Imat
23	Jul_cum>Iflo-Idrp	52	MaxTemp_avg_Ilev-Imat	81	Inn_min>Iflo-Imat
24	Raint_cum_Ilev-Imat	53	MaxTemp_avg>Iflo-Imat	82	Inn_min_Idrp-Imat
25	Raint_cum>Iflo-Imat	54	MaxTemp_avg_Idrp-Imat	83	Inn_min>Iflo-Idrp
26	Raint_cum_Idrp-Imat	55	MaxTemp_avg>Iflo-Idrp	84	Days_Inn_0.6_Ilev-Imat
27	Raint_cum>Iflo-Idrp	56	MaxTemp_max_Ilev-Imat	85	Days_Inn_0.6>Iflo-Imat
28	Etp(n)_cum_Ilev-Imat	57	MaxTemp_max>Iflo-Imat	86	Days_Inn_0.6_Idrp-Imat
29	Etp(n)_cum>Iflo-Imat	58	MaxTemp_max_Idrp-Imat	87	Days_Inn_0.6>Iflo-Idrp

**Table A2.** Name of variables processed from Multidisciplinary Simulator for Standard Crops (STICS). Crop phenology stages: Ilev (emergence), Idrp (grain filling onset), Iflo (flowering), Imat (physiological maturity); descriptive values: cum (cumulative), max (maximum), avg (average); thresholds (MinTemp, MaxTemp, Swfac, Inn variables)

## APPENDIX B

Pos	Variable name	Var Importance	Pos	Variable name	Var Importance
1	Masec(n)_Imat	0.7923	45	Inn_avg>Iflo-Idrp	0.3542
2	Lai(n)_Imat	0.7726	46	MinTemp_avg_Ilev-Imat	0.3508
3	Qnplante_Idrp	0.7710	47	Days_MaxTemp_28>Iflo-Imat	0.3478
4	Qnplante_Imat	0.7523	48	Precip_cum>Iflo-Idrp	0.3460
5	Masec(n)_Idrp	0.7334	49	MaxTemp_avg>Iflo-Imat	0.3432
6	Ep_cum_Idrp-Imat	0.6819	50	Days_MinTemp_18>Iflo-Idrp	0.3327
7	Qfix_Imat	0.6805	51	Inn_avg>Iflo-Imat	0.3099
8	Ep_cum>Iflo-Imat	0.6650	52	MinTemp_avg>Iflo-Idrp	0.2944
9	Raint_cum_Idrp-Imat	0.6326	53	Inn_avg_Ilev-Imat	0.2924
10	Lai(n)_Idrp	0.6292	54	Days_Inn_0.6>Iflo-Imat	0.2923
11	AvgTemp_avg_Idrp-Imat	0.6157	55	Days_Inn_0.6>Iflo-Idrp	0.2923
12	Swfac_avg>Iflo-Imat	0.6088	56	Days_Inn_0.6_Ilev-Imat	0.2903
13	MinTemp_avg_Idrp-Imat	0.5937	57	Inn_min>Iflo-Imat	0.2824
14	Ep_cum_Ilev-Imat	0.5842	58	Inn_min>Iflo-Idrp	0.2684
15	Days_Swfac_0.6>Iflo-Imat	0.5811	59	Inn_min_Idrp-Imat	0.2673
16	MinTemp_avg>Iflo-Imat	0.5654	60	Precip_cum_Idrp-Imat	0.2453
17	Swfac_min_Idrp-Imat	0.5638	61	Inn_min_Ilev-Imat	0.2405
18	Days_MinTemp_18_Idrp-Imat	0.5618	62	AvgTemp_avg_Ilev-Imat	0.2320
19	Swfac_min>Iflo-Imat	0.5600	63	Jul_cum_Ilev-Imat	0.1721
20	MaxTemp_avg_Idrp-Imat	0.5578	64	Masec(n)_Iflo	0.1698
21	AvgTemp_avg>Iflo-Imat	0.5551	65	Lai(n)_Iflo	0.1594
22	Swfac_min_Ilev-Imat	0.5521	66	MaxTemp_max_Ilev-Imat	0.1560
23	Days_MinTemp_18>Iflo-Imat	0.5328	67	Inn_avg_Idrp-Imat	0.1557
24	Days_MaxTemp_28_Idrp-Imat	0.5119	68	Days_MaxTemp_28_Ilev-Imat	0.1442
25	Ep_cum>Iflo-Idrp	0.5113	69	AvgTemp_avg>Iflo-Idrp	0.1030
26	Jul_cum_Idrp-Imat	0.5069	70	Zrac>Iflo	0.0934
27	Swfac_avg_Ilev-Imat	0.5054	71	Etp(n)_cum_Idrp-Imat	0.0858
28	Qfix_Idrp	0.4953	72	MaxTemp_avg>Iflo-Idrp	0.0856
29	Swfac_avg_Idrp-Imat	0.4929	73	Qfix>Iflo	0.0821
30	Swfac_avg>Iflo-Idrp	0.4909	74	Nbgrmax	0.0781
31	Days_Swfac_0.6_Ilev-Imat	0.4899	75	MaxTemp_max>Iflo-Imat	0.0773
32	Days_Swfac_0.6>Iflo-Idrp	0.4834	76	Etp(n)_cum_Ilev-Imat	0.0708
33	Raint_cum>Iflo-Imat	0.4712	77	Etp(n)_cum>Iflo-Imat	0.0701
34	Days_Swfac_0.6_Idrp-Imat	0.4627	78	Days_MaxTemp_28>Iflo-Idrp	0.0643
35	Zrac_Idrp	0.4592	79	MaxTemp_max>Iflo-Idrp	0.0618
36	Zrac_Imat	0.4536	80	MaxTemp_avg_Ilev-Imat	0.0613
37	Swfac_min>Iflo-Idrp	0.4464	81	Etp(n)_cum>Iflo-Idrp	0.0565
38	MaxTemp_max_Idrp-Imat	0.4257	82	Raint_cum>Iflo-Idrp	0.0461
39	Jul_cum>Iflo-Imat	0.3997	83	Jul_cum>Iflo-Idrp	0.0456
40	Days_MinTemp_18_Ilev-Imat	0.3926	84	Stflodrp	0.0372
41	Qnplante>Iflo	0.3866	85	Stlevdrp	0.0308
42	Raint_cum_Ilev-Imat	0.3802	86	Stdrpmat	0.0074
43	Precip_cum_Ilev-Imat	0.3714	87	Days_Inn_0.6_Idrp-Imat	0.0000
44	Precip_cum>Iflo-Imat	0.3585			

**Table B1.** Ranking of variables computed by Pearson correlation.

Pos	Variable name	Var Importance	Pos	Variable name	Var Importance
1	Lai(n)_Imat	0.7699	45	Precip_cum_Iflo-Imat	0.3140
2	Masec(n)_Imat	0.7311	46	Days_MinTemp_18_Iflo-Idrp	0.3018
3	Qnplante_Idrp	0.7137	47	Inn_avg_Iflo-Idrp	0.2983
4	Masec(n)_Idrp	0.7003	48	MinTemp_avg_Ilev-Imat	0.2851
5	Ep_cum_Iflo-Imat	0.6886	49	Inn_min_Idrp-Imat	0.2817
6	Ep_cum_Idrp-Imat	0.6734	50	Precip_cum_Ilev-Imat	0.2602
7	Qnplante_Imat	0.6714	51	Days_Inn_0.6_Ilev-Imat	0.2599
8	Ep_cum_Ilev-Imat	0.6456	52	Days_Inn_0.6_Iflo-Imat	0.2599
9	Lai(n)_Idrp	0.6439	53	Days_Inn_0.6_Iflo-Idrp	0.2599
10	Raint_cum_Idrp-Imat	0.6288	54	Inn_avg_Iflo-Imat	0.2570
11	Swfac_min_Idrp-Imat	0.6160	55	Precip_cum_Iflo-Idrp	0.2407
12	Swfac_min_Iflo-Imat	0.6136	56	Inn_min_Iflo-Idrp	0.2370
13	AvgTemp_avg_Idrp-Imat	0.6081	57	Inn_avg_Ilev-Imat	0.2353
14	Swfac_min_Ilev-Imat	0.6009	58	MinTemp_avg_Iflo-Idrp	0.2174
15	MinTemp_avg_Idrp-Imat	0.5977	59	Masec(n)_Iflo	0.2164
16	Qfix_Imat	0.5964	60	Inn_min_Iflo-Imat	0.2155
17	MaxTemp_avg_Idrp-Imat	0.5937	61	Lai(n)_Iflo	0.2105
18	Days_MinTemp_18_Idrp-Imat	0.5876	62	Inn_min_Ilev-Imat	0.1991
19	MinTemp_avg_Iflo-Imat	0.5758	63	Jul_cum_Ilev-Imat	0.1979
20	Swfac_avg_Iflo-Imat	0.5655	64	Days_MaxTemp_28_Ilev-Imat	0.1840
21	AvgTemp_avg_Iflo-Imat	0.5548	65	AvgTemp_avg_Ilev-Imat	0.1831
22	Days_MinTemp_18_Iflo-Imat	0.5510	66	MaxTemp_max_Ilev-Imat	0.1801
23	Ep_cum_Iflo-Idrp	0.5482	67	Inn_avg_Idrp-Imat	0.1667
24	Jul_cum_Idrp-Imat	0.5380	68	Precip_cum_Idrp-Imat	0.1519
25	Days_Swfac_0.6_Iflo-Imat	0.5361	69	AvgTemp_avg_Iflo-Idrp	0.1400
26	Days_MaxTemp_28_Idrp-Imat	0.5033	70	Qfix_Iflo	0.1263
27	Qfix_Idrp	0.4679	71	Nbgrmax	0.1160
28	Jul_cum_Iflo-Imat	0.4667	72	Etpp(n)_cum_Idrp-Imat	0.1095
29	MaxTemp_max_Idrp-Imat	0.4629	73	Raint_cum_Iflo-Idrp	0.1015
30	Raint_cum_Iflo-Imat	0.4590	74	MaxTemp_max_Iflo-Imat	0.0949
31	Days_Swfac_0.6_Ilev-Imat	0.4546	75	Jul_cum_Iflo-Idrp	0.0849
32	Swfac_avg_Ilev-Imat	0.4364	76	MaxTemp_avg_Ilev-Imat	0.0763
33	Swfac_avg_Idrp-Imat	0.4319	77	Etpp(n)_cum_Ilev-Imat	0.0763
34	Raint_cum_Ilev-Imat	0.4209	78	Etpp(n)_cum_Iflo-Idrp	0.0736
35	Qnplante_Iflo	0.4206	79	Etpp(n)_cum_Iflo-Imat	0.0731
36	Days_Swfac_0.6_Idrp-Imat	0.4148	80	Zrac_Iflo	0.0720
37	Swfac_avg_Iflo-Idrp	0.4131	81	Days_MaxTemp_28_Iflo-Idrp	0.0538
38	Swfac_min_Iflo-Idrp	0.4105	82	Stflodrp	0.0465
39	Days_Swfac_0.6_Iflo-Idrp	0.3993	83	MaxTemp_avg_Iflo-Idrp	0.0345
40	Days_MinTemp_18_Ilev-Imat	0.3857	84	MaxTemp_max_Iflo-Idrp	0.0235
41	Days_MaxTemp_28_Iflo-Imat	0.3552	85	Stlevdrp	0.0085
42	Zrac_Idrp	0.3287	86	Stdrpmat	0.0085
43	MaxTemp_avg_Iflo-Imat	0.3273	87	Days_Inn_0.6_Idrp-Imat	0.0000
44	Zrac_Imat	0.3214			

**Table B2.** Ranking of variables computed by Spearman correlation filter.



Pos	Variable name	Var Importance	Pos	Variable name	Var Importance
1	Lai(n)_Imat	0.5929	45	Inn_min_Iflo-Imat	0.1745
2	Masec(n)_Imat	0.5875	46	Inn_avg_Idrp-Imat	0.1744
3	Qnplante_Imat	0.5515	47	MinTemp_avg_Iflo-Imat	0.1687
4	Ep_cum_Idrp-Imat	0.4223	48	Inn_min_Idrp-Imat	0.1673
5	Qfix_Imat	0.4072	49	Days_Swfac_0.6_Ilev-Imat	0.1628
6	Inn_min_Iflo-Idrp	0.3799	50	Days_MaxTemp_28_Ilev-Imat	0.1595
7	Inn_avg_Iflo-Idrp	0.3652	51	Lai(n)_Iflo	0.1540
8	Ep_cum_Iflo-Imat	0.3486	52	Precip_cum_Ilev-Imat	0.1213
9	Days_Swfac_0.6_Iflo-Imat	0.3443	53	AvgTemp_avg_Ilev-Imat	0.1204
10	Inn_avg_Ilev-Imat	0.3400	54	MaxTemp_avg_Ilev-Imat	0.1204
11	Inn_avg_Iflo-Imat	0.3380	55	Etp(n)_cum_Iflo-Imat	0.0993
12	Masec(n)_Idrp	0.3300	56	Etp(n)_cum_Ilev-Imat	0.0993
13	Qnplante_Idrp	0.3285	57	Etp(n)_cum_Iflo-Idrp	0.0993
14	Raint_cum_Idrp-Imat	0.3080	58	Masec(n)_Iflo	0.0000
15	Days_Swfac_0.6_Iflo-Idrp	0.3025	59	Qfix_Iflo	0.0000
16	Precip_cum_Iflo-Imat	0.2988	60	Zrac_Iflo	0.0000
17	Qnplante_Iflo	0.2895	61	Etp(n)_cum_Idrp-Imat	0.0000
18	Ep_cum_Ilev-Imat	0.2833	62	Precip_cum_Idrp-Imat	0.0000
19	Swfac_avg_Iflo-Imat	0.2758	63	MaxTemp_avg_Iflo-Imat	0.0000
20	Lai(n)_Idrp	0.2711	64	MaxTemp_max_Iflo-Imat	0.0000
21	Swfac_min_Iflo-Imat	0.2476	65	Raint_cum_Ilev-Imat	0.0000
22	Swfac_min_Ilev-Imat	0.2476	66	MinTemp_avg_Ilev-Imat	0.0000
23	Zrac_Idrp	0.2457	67	Swfac_avg_Ilev-Imat	0.0000
24	Zrac_Imat	0.2457	68	MaxTemp_max_Ilev-Imat	0.0000
25	MinTemp_avg_Idrp-Imat	0.2374	69	Inn_min_Ilev-Imat	0.0000
26	Swfac_min_Iflo-Idrp	0.2309	70	Jul_cum_Ilev-Imat	0.0000
27	Swfac_min_Idrp-Imat	0.2289	71	Raint_cum_Iflo-Idrp	0.0000
28	AvgTemp_avg_Iflo-Imat	0.2266	72	AvgTemp_avg_Iflo-Idrp	0.0000
29	MaxTemp_avg_Idrp-Imat	0.2222	73	MinTemp_avg_Iflo-Idrp	0.0000
30	Days_MinTemp_18_Ilev-Imat	0.2214	74	MaxTemp_avg_Iflo-Idrp	0.0000
31	Jul_cum_Iflo-Imat	0.2191	75	MaxTemp_max_Iflo-Idrp	0.0000
32	Days_MinTemp_18_Iflo-Imat	0.2063	76	Jul_cum_Iflo-Idrp	0.0000
33	AvgTemp_avg_Idrp-Imat	0.2049	77	Days_Inn_0.6_Ilev-Imat	0.0000
34	Days_MinTemp_18_Idrp-Imat	0.2035	78	Days_MaxTemp_28_Iflo-Imat	0.0000
35	MaxTemp_max_Idrp-Imat	0.2000	79	Days_Inn_0.6_Iflo-Imat	0.0000
36	Qfix_Idrp	0.1980	80	Days_Inn_0.6_Idrp-Imat	0.0000
37	Ep_cum_Iflo-Idrp	0.1971	81	Days_MinTemp_18_Iflo-Idrp	0.0000
38	Jul_cum_Idrp-Imat	0.1969	82	Days_MaxTemp_28_Iflo-Idrp	0.0000
39	Days_MaxTemp_28_Idrp-Imat	0.1954	83	Days_Inn_0.6_Iflo-Idrp	0.0000
40	Raint_cum_Iflo-Imat	0.1927	84	Nbgrmax	0.0000
41	Swfac_avg_Idrp-Imat	0.1883	85	Stlevdrp	0.0000
42	Days_Swfac_0.6_Idrp-Imat	0.1883	86	Stflodrp	0.0000
43	Precip_cum_Iflo-Idrp	0.1872	87	Stdrrpmat	0.0000
44	Swfac_avg_Iflo-Idrp	0.1829			

**Table B3.** Ranking of variables computed by filter of entropy-based information gain.

## APPENDIX C

### Coefficients of linear regression created by LASSO

#	Variable name	Coefficient value	#	Variable name	Coefficient value
1	Masec(n)_Iflo	2.8188e+00	34	Inn_min_Iflo-Imat	-1.3651e+01
2	Lai(n)_Iflo	9.3241e-01	35	Raint_cum_Ilev-Imat	-1.1394e-02
3	Qnplante_Iflo	7.4166e-02	36	Precip_cum_Ilev-Imat	5.6827e-03
4	Qfix_Iflo	-1.7155e-01	37	Ep_cum_Ilev-Imat	-7.9358e-02
5	Zrac_Iflo	7.6535e-02	38	MinTemp_avg_Ilev-Imat	1.2562e-01
6	Masec(n)_Idrp	-4.0427e-01	39	MaxTemp_avg_Ilev-Imat	-3.7455e-04
7	Lai(n)_Idrp	7.3189e-01	40	Swfac_avg_Ilev-Imat	6.1859e+00
8	Qnplante_Idrp	-9.3804e-02	41	Inn_avg_Ilev-Imat	1.6985e+01
9	Qfix_Idrp	9.1514e-02	42	MaxTemp_max_Ilev-Imat	7.1837e-01
10	Zrac_Idrp	5.0038e-02	43	Swfac_min_Ilev-Imat	1.4684e-01
11	Masec(n)_Imat	5.1417e-01	44	Inn_min_Ilev-Imat	-3.9823e+00
12	Lai(n)_Imat	-4.0912e-01	45	Jul_cum_Ilev-Imat	-7.5989e-02
13	Qnplante_Imat	3.8100e-02	46	Precip_cum_Iflo-Idrp	6.9931e-03
14	Qfix_Imat	-5.2369e-02	47	Ep_cum_Iflo-Idrp	2.4697e-02
15	Zrac_Imat	-6.7964e-02	48	MinTemp_avg_Iflo-Idrp	3.9772e+00
16	Raint_cum_Idrp-Imat	9.6513e-03	49	MaxTemp_avg_Iflo-Idrp	-2.6303e+00
17	Precip_cum_Idrp-Imat	-2.8790e-03	50	Swfac_avg_Iflo-Idrp	1.6022e+01
18	MinTemp_avg_Idrp-Imat	4.7465e+00	51	Inn_avg_Iflo-Idrp	1.1904e+01
19	MaxTemp_avg_Idrp-Imat	-3.7388e+00	52	MaxTemp_max_Iflo-Idrp	-8.1299e-01
20	Swfac_avg_Idrp-Imat	1.2500e+01	53	Swfac_min_Iflo-Idrp	-4.1521e-01
21	Inn_avg_Idrp-Imat	3.1469e+01	54	Inn_min_Iflo-Idrp	2.0532e+01
22	MaxTemp_max_Idrp-Imat	-4.1193e-01	55	Jul_cum_Iflo-Idrp	4.9970e-01
23	Swfac_min_Idrp-Imat	-1.3343e+00	56	Days_MinTemp_18_Ilev-Imat	1.8624e-02
24	Inn_min_Idrp-Imat	-1.2703e+00	57	Days_MaxTemp_28_Ilev-Imat	4.6168e-02
25	Jul_cum_Idrp-Imat	-2.3218e-01	58	Days_Swfac_0.6_Ilev-Imat	3.6354e-03
26	Raint_cum_Iflo-Imat	5.7320e-03	59	Days_MinTemp_18_Iflo-Imat	-2.3197e-02
27	Ep_cum_Iflo-Imat	7.4176e-02	60	Days_MaxTemp_28_Iflo-Imat	-1.7790e-01
28	MinTemp_avg_Iflo-Imat	-9.4243e+00	61	Days_Swfac_0.6_Iflo-Imat	1.0801e-02
29	MaxTemp_avg_Iflo-Imat	7.7822e+00	62	Days_MinTemp_18_Iflo-Idrp	-1.0127e-01
30	Swfac_avg_Iflo-Imat	-2.8792e+01	63	Days_MaxTemp_28_Iflo-Idrp	-8.3875e-04
31	Inn_avg_Iflo-Imat	-4.6737e+01	64	Days_Swfac_0.6_Iflo-Idrp	5.2675e-03
32	MaxTemp_max_Iflo-Imat	-1.6202e-03	65	Nbgrmax	5.1039e-04
33	Swfac_min_Iflo-Imat	6.6187e-02	66	Stdrpmat	9.8675e-03

**Table C1.** Coefficients of linear regression created by LASSO. Coefficients equal to zero were assigned to 11 variables.

### Linear regressions created by M5 decision tree

#### Linear regression number 1:

$$Mafruit = -0.2193 * Lai(n)_Iflo + 0.0187 * Qnplante_Iflo - 0.0314 * Qfix_Iflo + 0.0869 * Lai(n)_Idrp + 0.0759 * Masec(n)_Imat + 0.002 * Qfix_Imat + 3.9514 * Inn_avg_Iflo-Idrp - 1.665 * Inn_min_Iflo-Idrp - 1.0665$$

#### Linear regression number 2:

$$Mafruit = -0.243 * Masec(n)_Iflo - 0.2193 * Lai(n)_Iflo + 0.0305 * Qnplante_Iflo - 0.0179 * Qfix_Iflo + 0.0047 * Zrac_Iflo + 0.0869 * Lai(n)_Idrp + 0.0434 * Masec(n)_Imat + 0.002 * Qfix_Imat + 0.0036 * Ep_cum_Idrp-Imat + 0.0287 * MaxTemp_avg_Ilev-Imat + 3.2551 * Inn_avg_Iflo-Idrp - 1.665 * Inn_min_Iflo-Idrp - 1.7154$$

**Linear regression number 3:**

$$\begin{aligned} Mafruit = & -0.4282 * Masec(n)_{Iflo} - 0.2193 * Lai(n)_{Iflo} + 0.0242 * Qnplante_{Iflo} - 0.0398 * Qfix_{Iflo} + 0.0869 \\ & * Lai(n)_{Idrp} + 0.0434 * Masec(n)_{Imat} + 0.002 * Qfix_{Imat} + 0.0032 * Ep_{cum\_Idrp-Imat} + 0.0258 * \\ & MaxTemp_{avg\_Ilev-Imat} + 3.2551 * Inn_{avg\_Iflo-Idrp} - 1.665 * Inn_{min\_Iflo-Idrp} - 0.1411 \end{aligned}$$

**Linear regression number 4:**

$$\begin{aligned} Mafruit = & -0.4282 * Masec(n)_{Iflo} - 0.2193 * Lai(n)_{Iflo} + 0.0242 * Qnplante_{Iflo} - 0.0398 * Qfix_{Iflo} + 0.0869 \\ & * Lai(n)_{Idrp} + 0.0434 * Masec(n)_{Imat} + 0.002 * Qfix_{Imat} + 0.0032 * Ep_{cum\_Idrp-Imat} + 0.0258 * \\ & MaxTemp_{avg\_Ilev-Imat} + 3.2551 * Inn_{avg\_Iflo-Idrp} - 1.665 * Inn_{min\_Iflo-Idrp} - 0.1438 \end{aligned}$$

**Linear regression number 5:**

$$\begin{aligned} Mafruit = & -0.4587 * Masec(n)_{Iflo} - 0.2193 * Lai(n)_{Iflo} + 0.0242 * Qnplante_{Iflo} - 0.0401 * Qfix_{Iflo} + 0.0869 \\ & * Lai(n)_{Idrp} + 0.0434 * Masec(n)_{Imat} + 0.002 * Qfix_{Imat} + 0.0032 * Ep_{cum\_Idrp-Imat} + 0.0258 * \\ & MaxTemp_{avg\_Ilev-Imat} + 3.2551 * Inn_{avg\_Iflo-Idrp} - 1.665 * Inn_{min\_Iflo-Idrp} - 0.0967 \end{aligned}$$

**Linear regression number 6:**

$$\begin{aligned} Mafruit = & -0.3026 * Masec(n)_{Iflo} - 0.2193 * Lai(n)_{Iflo} + 0.0242 * Qnplante_{Iflo} - 0.0312 * Qfix_{Iflo} + 0.0869 \\ & * Lai(n)_{Idrp} + 0.0434 * Masec(n)_{Imat} + 0.002 * Qfix_{Imat} + 0.0032 * Ep_{cum\_Idrp-Imat} + 0.0258 * \\ & MaxTemp_{avg\_Ilev-Imat} + 3.2551 * Inn_{avg\_Iflo-Idrp} - 1.665 * Inn_{min\_Iflo-Idrp} - 0.5323 \end{aligned}$$

**Linear regression number 7:**

$$\begin{aligned} Mafruit = & -0.2811 * Masec(n)_{Iflo} + 0.0803 * Lai(n)_{Iflo} + 0.0067 * Qnplante_{Iflo} + 0.0383 * Qfix_{Iflo} + 0.0881 \\ & * Masec(n)_{Idrp} + 0.0103 * Lai(n)_{Idrp} + 0.0017 * Qfix_{Imat} - 0.0046 * Ep_{cum\_Idrp-Imat} + 0.7974 * \\ & Swfac_{avg\_Idrp-Imat} + 0.577 * Swfac_{avg\_Iflo-Imat} + 3.8547 * Inn_{avg\_Iflo-Idrp} - 2.4314 * Inn_{min\_Iflo-Idrp} \\ & + 0.256 \end{aligned}$$

**Linear regression number 8:**

$$\begin{aligned} Mafruit = & -0.1899 * Masec(n)_{Iflo} + 0.0274 * Lai(n)_{Iflo} + 0.0067 * Qnplante_{Iflo} + 0.0223 * Qfix_{Iflo} + 0.0881 \\ & * Masec(n)_{Idrp} + 0.0256 * Lai(n)_{Idrp} + 0.0017 * Qfix_{Imat} - 0.0041 * Ep_{cum\_Idrp-Imat} + 0.7974 * \\ & Swfac_{avg\_Idrp-Imat} + 0.6392 * Swfac_{avg\_Iflo-Imat} + 3.8547 * Inn_{avg\_Iflo-Idrp} - 2.4314 * Inn_{min\_Iflo-Idrp} \\ & + 0.1624 \end{aligned}$$

**Linear regression number 9:**

$$\begin{aligned} Mafruit = & -0.1928 * Masec(n)_{Iflo} + 0.0274 * Lai(n)_{Iflo} + 0.0067 * Qnplante_{Iflo} + 0.0223 * Qfix_{Iflo} + 0.0881 \\ & * Masec(n)_{Idrp} + 0.0256 * Lai(n)_{Idrp} + 0.0017 * Qfix_{Imat} - 0.0041 * Ep_{cum\_Idrp-Imat} + 0.7974 * \\ & Swfac_{avg\_Idrp-Imat} + 0.6669 * Swfac_{avg\_Iflo-Imat} + 3.8547 * Inn_{avg\_Iflo-Idrp} - 2.4314 * Inn_{min\_Iflo-Idrp} \\ & + 0.1587 \end{aligned}$$

**Linear regression number 10:**

$$\begin{aligned} Mafruit = & -0.1928 * Masec(n)_{Iflo} + 0.0274 * Lai(n)_{Iflo} + 0.0067 * Qnplante_{Iflo} + 0.0223 * Qfix_{Iflo} + 0.0881 \\ & * Masec(n)_{Idrp} + 0.0256 * Lai(n)_{Idrp} + 0.0017 * Qfix_{Imat} - 0.0041 * Ep_{cum\_Idrp-Imat} + 0.7974 * \\ & Swfac_{avg\_Idrp-Imat} + 0.3752 * Swfac_{avg\_Iflo-Imat} + 3.8547 * Inn_{avg\_Iflo-Idrp} - 2.4314 * Inn_{min\_Iflo-Idrp} \\ & + 0.3922 \end{aligned}$$

**Linear regression number 11:**

$$\begin{aligned} Mafruit = & -0.163 * Masec(n)_{Iflo} - 0.2727 * Lai(n)_{Iflo} + 0.0067 * Qnplante_{Iflo} + 0.0228 * Qfix_{Iflo} + 0.0881 \\ & * Masec(n)_{Idrp} + 0.0528 * Lai(n)_{Idrp} + 0.0017 * Qfix_{Imat} - 0.0032 * Ep_{cum\_Idrp-Imat} + 1.002 * \\ & Swfac_{avg\_Idrp-Imat} + 0.1212 * Swfac_{avg\_Iflo-Imat} + 3.8547 * Inn_{avg\_Iflo-Idrp} - 2.0948 * Inn_{min\_Iflo-Idrp} \\ & + 0.6173 \end{aligned}$$

**Linear regression number 12:**

$$\begin{aligned} \text{Mafruit} = & -0.163 * \text{Masec}(n)\_Iflo - 0.1797 * \text{Lai}(n)\_Iflo + 0.0067 * \text{Qnplante\_Iflo} + 0.0234 * \text{Qfix\_Iflo} + 0.0881 \\ & * \text{Masec}(n)\_Idrp + 0.0528 * \text{Lai}(n)\_Idrp + 0.0017 * \text{Qfix\_Imat} - 0.0032 * \text{Ep\_cum\_Idrp-Imat} + 1.0215 * \\ & \text{Swfac\_avg\_Idrp-Imat} + 0.1212 * \text{Swfac\_avg\_Iflo-Imat} + 3.8547 * \text{Inn\_avg\_Iflo-Idrp} - 2.0948 * \text{Inn\_min\_Iflo-Idrp} \\ & + 0.3868 \end{aligned}$$

**Linear regression number 13:**

$$\begin{aligned} \text{Mafruit} = & -0.0608 * \text{Lai}(n)\_Iflo + 0.0067 * \text{Qnplante\_Iflo} + 0.0881 * \text{Masec}(n)\_Idrp + 0.0528 * \text{Lai}(n)\_Idrp + \\ & 0.0017 * \text{Qfix\_Imat} - 0.0032 * \text{Ep\_cum\_Idrp-Imat} + 0.7974 * \text{Swfac\_avg\_Idrp-Imat} + 0.0005 * \text{Precip\_cum\_Iflo-Imat} \\ & + 0.1593 * \text{Swfac\_avg\_Iflo-Imat} + 5.2879 * \text{Inn\_avg\_Iflo-Idrp} - 4.1489 * \text{Inn\_min\_Iflo-Idrp} + 0.3625 \end{aligned}$$

**Linear regression number 14:**

$$\begin{aligned} \text{Mafruit} = & -0.0608 * \text{Lai}(n)\_Iflo + 0.0067 * \text{Qnplante\_Iflo} + 0.102 * \text{Masec}(n)\_Idrp + 0.0528 * \text{Lai}(n)\_Idrp + \\ & 0.0017 * \text{Qfix\_Imat} - 0.0032 * \text{Ep\_cum\_Idrp-Imat} + 0.7974 * \text{Swfac\_avg\_Idrp-Imat} + 0.0004 * \text{Precip\_cum\_Iflo-Imat} \\ & + 0.1593 * \text{Swfac\_avg\_Iflo-Imat} + 5.2879 * \text{Inn\_avg\_Iflo-Idrp} - 4.1489 * \text{Inn\_min\_Iflo-Idrp} + 0.3484 \end{aligned}$$

**Linear regression number 15:**

$$\begin{aligned} \text{Mafruit} = & -0.0608 * \text{Lai}(n)\_Iflo + 0.0067 * \text{Qnplante\_Iflo} + 0.1013 * \text{Masec}(n)\_Idrp + 0.0528 * \text{Lai}(n)\_Idrp + \\ & 0.0017 * \text{Qfix\_Imat} - 0.0032 * \text{Ep\_cum\_Idrp-Imat} + 0.7974 * \text{Swfac\_avg\_Idrp-Imat} + 0.0004 * \text{Precip\_cum\_Iflo-Imat} \\ & + 0.1593 * \text{Swfac\_avg\_Iflo-Imat} + 5.2879 * \text{Inn\_avg\_Iflo-Idrp} - 4.1489 * \text{Inn\_min\_Iflo-Idrp} + 0.36 \end{aligned}$$

**Linear regression number 16**

$$\begin{aligned} \text{Mafruit} = & 0.0227 * \text{Masec}(n)\_Iflo - 0.2846 * \text{Lai}(n)\_Iflo + 0.0067 * \text{Qnplante\_Iflo} + 0.0131 * \text{Qfix\_Iflo} + 0.2127 \\ & * \text{Masec}(n)\_Idrp + 0.0528 * \text{Lai}(n)\_Idrp + 0.0025 * \text{Qfix\_Imat} - 0.0077 * \text{Ep\_cum\_Idrp-Imat} + 1.9247 * \\ & \text{Swfac\_avg\_Idrp-Imat} - 1.1523 * \text{Swfac\_avg\_Iflo-Imat} + 4.2938 * \text{Inn\_avg\_Iflo-Idrp} - 3.7675 * \text{Inn\_min\_Iflo-Idrp} \\ & + 1.6917 \end{aligned}$$

**Linear regression number 17:**

$$\begin{aligned} \text{Mafruit} = & 0.0184 * \text{Masec}(n)\_Iflo - 0.2846 * \text{Lai}(n)\_Iflo + 0.0067 * \text{Qnplante\_Iflo} + 0.0131 * \text{Qfix\_Iflo} + 0.2127 \\ & * \text{Masec}(n)\_Idrp + 0.0528 * \text{Lai}(n)\_Idrp + 0.0025 * \text{Qfix\_Imat} - 0.0077 * \text{Ep\_cum\_Idrp-Imat} + 1.9247 * \\ & \text{Swfac\_avg\_Idrp-Imat} - 1.1523 * \text{Swfac\_avg\_Iflo-Imat} + 4.2938 * \text{Inn\_avg\_Iflo-Idrp} - 3.7675 * \text{Inn\_min\_Iflo-Idrp} \\ & + 1.7071 \end{aligned}$$

**Linear regression number 18:**

$$\begin{aligned} \text{Mafruit} = & -0.2114 * \text{Masec}(n)\_Iflo - 0.2846 * \text{Lai}(n)\_Iflo + 0.0067 * \text{Qnplante\_Iflo} + 0.0143 * \text{Qfix\_Iflo} + 0.2127 \\ & * \text{Masec}(n)\_Idrp + 0.0528 * \text{Lai}(n)\_Idrp + 0.0025 * \text{Qfix\_Imat} - 0.0077 * \text{Ep\_cum\_Idrp-Imat} + 1.9247 * \\ & \text{Swfac\_avg\_Idrp-Imat} - 1.1523 * \text{Swfac\_avg\_Iflo-Imat} + 4.2938 * \text{Inn\_avg\_Iflo-Idrp} - 3.7675 * \text{Inn\_min\_Iflo-Idrp} \\ & + 2.2973 \end{aligned}$$

**Linear regression number 19:**

$$\begin{aligned} \text{Mafruit} = & -0.1891 * \text{Masec}(n)\_Iflo - 0.2846 * \text{Lai}(n)\_Iflo + 0.0067 * \text{Qnplante\_Iflo} + 0.0143 * \text{Qfix\_Iflo} + 0.2127 \\ & * \text{Masec}(n)\_Idrp + 0.0528 * \text{Lai}(n)\_Idrp + 0.0025 * \text{Qfix\_Imat} - 0.0077 * \text{Ep\_cum\_Idrp-Imat} + 1.9247 * \\ & \text{Swfac\_avg\_Idrp-Imat} - 1.1523 * \text{Swfac\_avg\_Iflo-Imat} + 4.2938 * \text{Inn\_avg\_Iflo-Idrp} - 3.7675 * \text{Inn\_min\_Iflo-Idrp} \\ & + 2.2385 \end{aligned}$$